2012-03

Nowcasting Hail Size for Non-Supercell Thunderstorms in the Northeastern U. S.

Hasa; J., Petrit

Monterey, California. Naval Postgraduate School

NAVAL POSTGRADUATE SCHOOL

MONTEREY, CALIFORNIA

THESIS

NOWCASTING HAIL SIZE FOR NON-SUPERCELL THUNDERSTORMS IN THE NORTHEASTERN U.S.

by

Petrit J. Hasa

March 2012

Thesis Advisor: Wendell A. Nuss
Second Reader: Michael M. Bell

Approved for public release; distribution is unlimited

THIS PAGE INTENTIONALLY LEFT BLANK

REPORT DOCUMENTATION PAGE			Form Approved OMB No. 0704–0188
Public reporting burden for this collection of information is estimated to average 1 hour per response, including the time for reviewing instruction, searching existing data sources, gathering and maintaining the data needed, and completing and reviewing the collection of information. Send comments regarding this burden estimate or any other aspect of this collection of information, including suggestions for reducing this burden, to Washington headquarters Services, Directorate for Information Operations and Reports, 1215 Jefferson Davis Highway, Suite 1204, Arlington, VA 22202–4302, and to the Office of Management and Budget, Paperwork Reduction Project (0704–0188) Washington DC 20503.			
1. AGENCY USE ONLY ***(Leave blank)***	**2. REPORT DATE** March 2012	**3. REPORT TYPE AND DATES COVERED** Master's Thesis	
4. TITLE AND SUBTITLE Nowcasting Hail Size for Non-Supercell Thunderstorms in the Northeastern U. S.		**5. FUNDING NUMBERS**	
6. AUTHOR(S) Hasa, Petrit J.			
7. PERFORMING ORGANIZATION NAME(S) AND ADDRESS(ES) Naval Postgraduate School Monterey, CA 93943–5000		**8. PERFORMING ORGANIZATION REPORT NUMBER**	
9. SPONSORING /MONITORING AGENCY NAME(S) AND ADDRESS(ES) N/A		**10. SPONSORING/MONITORING AGENCY REPORT NUMBER**	
11. SUPPLEMENTARY NOTES The views expressed in this thesis are those of the author and do not reflect the official policy or position of the Department of Defense or the U.S. Government. IRB Protocol number _____N/A_____.			
12a. DISTRIBUTION / AVAILABILITY STATEMENT Approved for public release; distribution is unlimited		**12b. DISTRIBUTION CODE**	

13. ABSTRACT (maximum 200 words)

Hail size prediction is a difficult task for meteorologists. The most recent method used by the United States Air Force after thunderstorm initiation involves identifying the amount of storm-top divergence and correlating that value to the height of the freezing level. However, this method was based on a study that looked at both supercell and multicell thunderstorms alike. This paper attempts to build off this previous study, although solely looking at non-supercell thunderstorms based on the hypothesis that due to dynamic differences between the storm types, common indicators found in both are not indicative that hail of similar size will be produced.

14. SUBJECT TERMS Freezing Level, Hail Size, Non-Supercell Thunderstorms, Northeastern U.S., Storm-top Divergence			**15. NUMBER OF PAGES** 77
			16. PRICE CODE
17. SECURITY CLASSIFICATION OF REPORT Unclassified	**18. SECURITY CLASSIFICATION OF THIS PAGE** Unclassified	**19. SECURITY CLASSIFICATION OF ABSTRACT** Unclassified	**20. LIMITATION OF ABSTRACT** UU

NSN 7540–01–280–5500 Standard Form 298 (Rev. 2–89)
Prescribed by ANSI Std. 239–18

THIS PAGE INTENTIONALLY LEFT BLANK

Approved for public release; distribution is unlimited

NOWCASTING HAIL SIZE FOR NON-SUPERCELL THUNDERSTORMS IN THE NORTHEASTERN U. S.

Petrit J. Hasa
Captain, United States Air Force
B.S., Valparaiso University, 2003

Submitted in partial fulfillment of the
requirements for the degree of

MASTER OF SCIENCE IN METEOROLOGY

from the

NAVAL POSTGRADUATE SCHOOL
MARCH 2012

Author: Petrit J. Hasa

Approved by: Wendell A. Nuss
Thesis Advisor

Michael M. Bell
Second Reader

Wendell A. Nuss
Chair, Department of Meteorology

THIS PAGE INTENTIONALLY LEFT BLANK

ABSTRACT

Hail size prediction is a difficult task for meteorologists. The most recent method used by the United States Air Force after thunderstorm initiation involves identifying the amount of storm-top divergence and correlating that value to the height of the freezing level. However, this method was based on a study that looked at both supercell and multicell thunderstorms alike. This paper attempts to build off this previous study, although solely looking at non-supercell thunderstorms based on the hypothesis that due to dynamic differences between the storm types, common indicators found in both are not indicative that hail of similar size will be produced.

THIS PAGE INTENTIONALLY LEFT BLANK

TABLE OF CONTENTS

THIS PAGE INTENTIONALLY LEFT BLANK

LIST OF FIGURES

LIST OF TABLES

THIS PAGE INTENTIONALLY LEFT BLANK

ACKNOWLEDGMENTS

I would like to thank my advisor, Professor Wendell A. Nuss, Chair, Department of Meteorology, Naval Postgraduate School. His meteorological expertise and support throughout the development of this thesis proved invaluable. I would also like to thank Professor Michael M. Bell, Research Assistant Professor, Department of Meteorology, Naval Postgraduate School, for serving as my second reader and for his expertise with radar interrogation software. His assistance ensured the analysis portion of this research moved along smoothly. Next, I would like to thank Mr. Robert Creasey, Staff Meteorology, Naval Postgraduate School, for providing me with all the necessary tools to complete my thesis.

Furthermore, I would like to thank Ms. Allison Wreath and Mr. Lawrence McCoy of the 15th Operational Weather Squadron, Scott Air Force Base, Illinois, for providing the topic of this research and for supplying initial guidance. I would also like to thank John Kobar, National Climatic Data Center, National Oceanic and Atmospheric Association, and both Tim Crum and Bill Greenwood, Radar Operations Center, National Oceanic and Atmospheric Association, for their assistance in obtaining radar data in the proper format for analysis.

Additionally, I would like to thank my parents, Qani and Linda, for supporting my passion for weather. Their guidance and encouragement enabled me to realize my goal to become a Meteorologist. Last but not least, I thank my wife, Tracy, for being by my side throughout my entire Air Force career, supporting me through all of my pursuits and goals as no one else has. Without her, none of this would have been possible.

THIS PAGE INTENTIONALLY LEFT BLANK

I. INTRODUCTION

Each year, hail produced from thunderstorms poses a threat to life and property all over the world. While forecasting thunderstorms that are capable of producing hail is a challenge in itself, the bigger challenge is identifying which storm will produce hail and how large the hailstones will be. Providing forecasters with proper knowledge and tools to accurately predict hailstone size produced by a thunderstorm would greatly reduce the impending risk to people and property in the path of the storm.

While hail from thunderstorms causes an inordinate amount of monetary damage in the United States each year, the aviation community has a specific interest in hail forecasting as hailstones are particularly hazardous to flying operations. The United States Air Force's (USAF) interest in the threat posed by hail is evidenced by the severe hail watch and warning criteria for each Air Force base, which typically requires four and two hour lead times respectively. Normally these watches and warnings are issued prior to storm initiation as the average thunderstorm lifespan is 30 minutes. However, only after convection has developed and radar signatures appear can hail size and location be predicted with any reasonable fidelity.

Once a thunderstorm has formed, the primary tool used to predict hail size and location is radar. Storm-top divergence has been a key parameter used to predict hail size since the fielding of the WSR-88D radar, however many more meteorological factors are involved in developing hailstones. Consequently, storm-top divergence alone is not an accurate gauge of the size of a hailstone produced by a thunderstorm. However, storm-top divergence derived from radar is as close to a direct measure of updraft strength and should serve as a useful hail forecast parameter. Parameters such as the height of the freezing level and wet bulb zero height have recently been utilized in conjunction with storm-top divergence to predict hail size.

Previous thunderstorm studies have typically focused on supercell thunderstorms that occur in the Great Plains and most approaches to relate storm-top divergence to hail are based on these types of storms. However, of all thunderstorms, supercells account for

a small amount and are not responsible for the majority of hail reports and forecast tools applicable to Great Plains supercells may not work in other regions. Additionally, thunderstorms occur in all regions of the United States, not just the Great Plains. Predicting hail size from thunderstorms occurring over the Northeastern U.S. has been particularly difficult for forecasters of the USAF's 15th Operational Weather Squadron (OWS). Therefore, the focus of this thesis is to interrogate non-supercell thunderstorms that occur in the Northeastern U.S. to determine whether the results discovered in previous studies can be applied to all thunderstorm types regardless of location. The overall goal is to develop a more region-specific tool for interpreting storm-top divergence to predict hail size for the Northeast U.S.

II. BACKGROUND

When discussing severe weather such as large hail, damaging winds and tornadoes, it is impulsive as meteorologists to think of supercell thunderstorms. Even though supercells are highly dangerous thunderstorms that are prone to producing severe weather, non-supercell thunderstorms also produce an immense amount of damaging wind, hail, and tornado events every year. Supercell thunderstorms are dynamically different from other types of thunderstorms, and key severe weather forecast parameters observed in both types of storms likely will result in different severe weather events of varying magnitude. Since most previous severe weather studies were primarily focused on supercells, the direct applications of forecast parameters to the other types of thunderstorms may not provide accurate guidance about their potential to produce severe weather.

Identifying the atmospheric conditions where the different types of thunderstorms often develop is important to help assess their potential to produce severe weather. While hailstones can be generated by all of the thunderstorm types, certain types of storms are more apt at producing very large hailstones as opposed to small hailstones that are not considered severe. The development and growth in size of hailstones is conceptually well understood but difficult to assess in an operational environment. Of particular importance, Donavon (2007) showed that the height of the freezing level plays an important role in the development of hail. More fundamental is the strength of the updraft as it is known to be important to produce hail. Lastly, recent research has attempted to correlate the radar parameter of storm-top divergence as a proxy for updraft strength to hailstone size. The importance of storm-top divergence and what the value implies about a thunderstorm will be explored, as well as the previous research connecting storm-top divergence to hail.

A. TYPES OF CONVECTIVE STORMS

As noted by Weisman and Klemp (1986) and Chaston (1999) many different types of thunderstorms can occur that are fundamentally different in their evolution and ability to produce hail. Thunderstorms, as observed on radar and by the human eye, display specific characteristics that allow all thunderstorms to be classified into different types. These include both individual storms and others that are classified as systems. There are three different types of individual thunderstorms; the single-cell storm, the multicell storm, and the supercell storm. There is also a wide array of thunderstorm systems, known as mesoscale convective systems. These include but are not limited to squall-lines, bow-echoes, and quasi-stationary mesoscale convective systems. The basic characteristics of these different types of storms will be reviewed in terms of their potential to produce severe weather.

The most common of all thunderstorms, and sometimes called airmass thunderstorms, the single-cell storm consists of a single updraft that rises rapidly through the troposphere. Figure 1 illustrates the life cycle of one of these storms. Usually not severe, they tend to have an average lifespan between 30 and 50 minutes, but can sometimes last over an hour. Some single-cell storms can produce severe weather, typically in the form of damaging winds or hail due to intense updraft speeds over 70 mph and high liquid water concentration within the updraft. The occurrence of severe weather tends to be short-lived and tornadoes are rare. For these types of systems the updraft strength is crucial for the production of hail of any significant size.

Multicell thunderstorms, illustrated in Figure 2, are composed of a cluster of single cells that are individually short-lived. Outflow from each cell combine to form a gust front, which triggers new convection, allowing new cells to evolve as mature ones decay or dissipate. Since each individual cell is responsible for producing hail, the updraft strength in individual cells will again be crucial to assess hail size. Because of their ability to renew themselves constantly through new cell growth, multicell storms may last a long time, affecting vast areas. The greatest percentage of severe thunderstorms are multicell type storms, although the most severe type of thunderstorm is the supercell type.

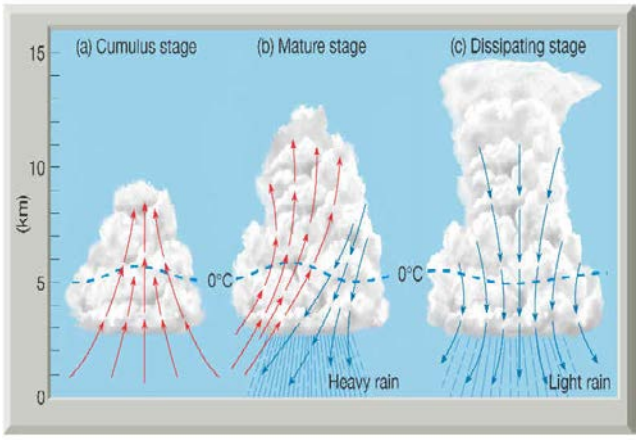

Figure 1. Single-cell or Airmass Thunderstorm characterized by the individual cell that is comprised of three short phases:
(a) cumulus, (b) mature, and (c) dissipating.
(Image from http://weatherblog.nbcactionnews.com/its-mothers-day-any t-storms-coming-our-way/)

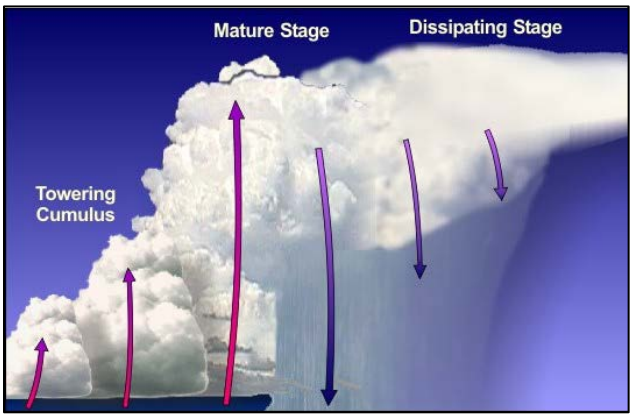

Figure 2. Multicell Thunderstorm comprised of a cluster of cells ranging in phase from initiation to dissipation.
(Image from http://www.srh.noaa.gov/jetstream/tstorms/ tstrmtypes.htm).

A supercell thunderstorm, which is illustrated in Figure 3, is an intense long-lived thunderstorm that causes the most severe of all convective weather. It may produce high winds, large hail, and long-lived tornadoes over a wide path. The supercell consists of a single rotating updraft, the rotation of which distinguishes the supercell as dynamically different from the other thunderstorm types. The more complex dynamics of a supercell thunderstorm result in a somewhat different mechanism for hail growth than simply

updraft strength. However, Boustead (2008) formed a reasonable correlation between hail size and storm-top divergence. Because of the dynamic differences, the single cell within the supercell can have a lifetime of several hours as opposed to the cells within the other individual storm types. The supercell itself has a typical life cycle of about three hours, sometimes lasting up to six hours.

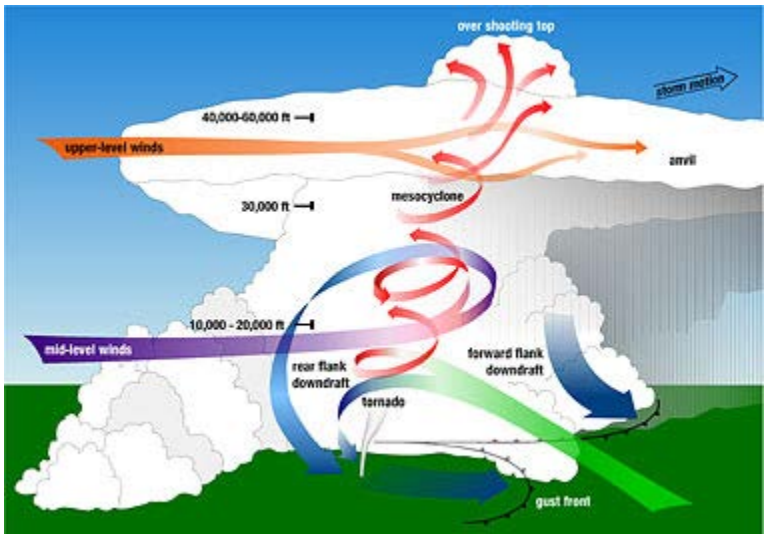

Figure 3. Supercell Thunderstorm, consisting of one long-lived rotating cell. (Image from http://www.nssl.noaa.gov/primer/tornado/tor_basics.html).

The squall-line is distinguishable from other storms or systems of storms by its continuity as a system. A squall-line, an example of which is shown in Figure 4, may be comprised of single-cell storms, multicell storms, or supercells in any combination. The cells a squall-line are oriented in a line that stretches for hundreds of miles. Consequently, the production of hail may follow similar patterns of development as individual storms. Squall-lines in the mid-latitudes are frequently associated with the cold front of a mid-latitude low pressure system. These squall-lines can develop along the cold front or up to a few hundred miles ahead of the front. Squall-lines can also be tropical in nature, but tropical storm systems rarely produce large hail due to warm and moist air throughout the entire vertical column of the troposphere.

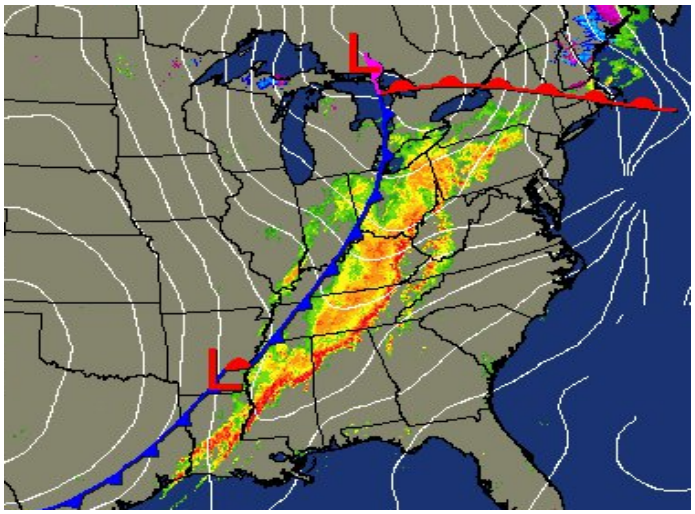

Figure 4. Squall-line of thunderstorms, typically found along or ahead of a cold front in the mid-latitudes. (Image from http://www.rellimzone.com/images/weather/current-weather-04–04–2011.jpg)

A bow-echo is similar to a squall-line in that it is a system of cells oriented into a line. However, the illustration in Figure 5 shows that the line of storms bows outward instead of resembling a straight line. A bow-echo can be a part of a squall-line or can be a line of thunderstorms itself. The main threat posed by a bow-echo is damaging straight line winds, although these organized storm systems can also produce both hail and tornadoes (see http://www.nws.noaa.gov/glossary, June 2009).

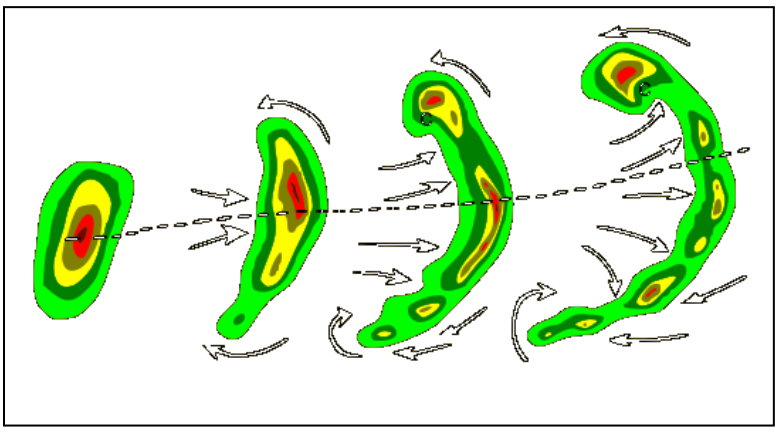

Figure 5. Bow Echo Thunderstorm, consisting of a small line of storms that "bows" in the middle. (Image from http://en.wikipedia.org/wiki/Bow_echo)

B. REQUIRED ATMOSPHERIC INGREDIENTS FOR THUNDERSTORMS

For thunderstorms to occur there are three necessary conditions for development; lift from a triggering mechanism, instability of the atmosphere, and moisture in the air (derived from Chaston 1999). The lifting or triggering components for thunderstorm development are characterized as dynamic lifting and mechanical lifting mechanisms. An example of a dynamic lifting mechanism is heating of the day, warming air at the surface which then rises. An example of a mechanical lifting mechanism is an advancing cold front, which pushes up warmer air just ahead of the front. Instability is defined as the tendency for air parcels to accelerate when they are displaced from their original position. The degree of instability depends upon the lapse rate of the environment compared to the parcel cooling rate, which determines the magnitude of the updraft.

Moisture is generally required in convection for two reasons. The first and most important reason is that without moisture, there would be no clouds. Secondly, moisture in the lower atmosphere generally adds to the instability of the vertical column. As mentioned above, instability occurs when a lifted parcel cools at a slower rate than that of the atmospheric lapse rate. If moisture is present in the parcel and the parcel becomes saturated as it cools, latent heat will be released into the parcel effectively slowing its rate of cooling. The process of latent heat release causes some lifted parcels to be warmer than the surrounding atmosphere—unstable—when they otherwise would have been cooler than the surrounding atmosphere—stable.

C. HAIL FORMATION AND PREDICTION

Hail is a common phenomenon within thunderstorms in the mid-latitudes. The popular theory begins with a small object, either a frozen raindrop or even an insect, which is lifted into the upper troposphere by the updraft of a thunderstorm where supercooled liquid is present. The supercooled liquid accumulates on the object and freezes, developing a hailstone. The updraft keeps the hailstone suspended in the air where it continues to grow through accretion. When the hailstone becomes too heavy to be held aloft or the hailstone is flung away from the updraft, the hailstone will fall to earth (Chaston 1999). While all thunderstorms in the mid-latitudes produce hail, most

hailstones generally do not reach the earth's surface. This is because hailstones melt as they fall through the lower troposphere where the temperatures are above freezing. Hailstones that reach the earth's surface only do so because they grow large enough to not melt completely during descent. See Figure 6 for an illustration of the hail formation process.

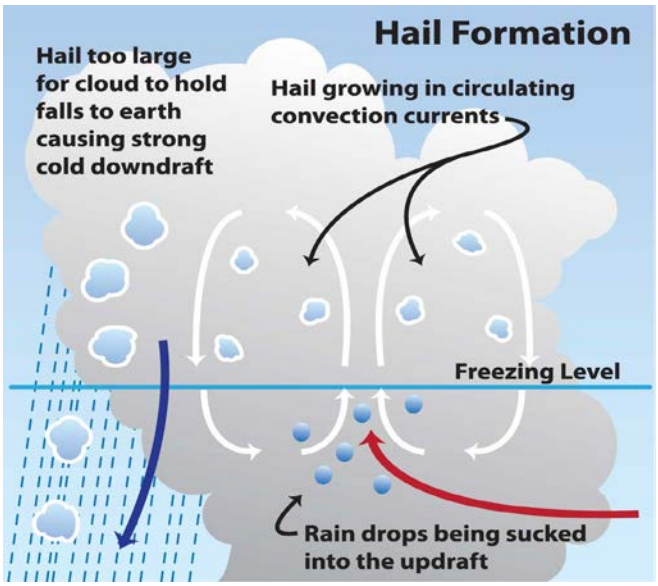

Figure 6. Formation of hail within a thunderstorm. The updraft lifts a small object above the freezing level where supercooled liquid solidifies on the object upon contact, forming hail. Growth continues until the hail is no longer sustained by an updraft.
(Image from http://scijinks.nasa.gov/_media/en/site/rain/hail-formation-large.jpg)

Hail formation is difficult to predict in detail, especially in terms that are accessible and useful to operational forecasters (Doswell 2000). One of the many methods used by operational forecasters to predict hail involves using the radar parameter of storm-top divergence and the height of the freezing level, as developed by Boustead (2008). The wet-bulb zero height is another parameter often used when discussing the possibility for severe hail.

Thunderstorms act to release convective instability through upward acceleration of air, which results in a pattern of horizontal convergence at low levels surmounted by

horizontal divergence at some higher level (Beebe and Bates 1954). When the updraft of a thunderstorm encounters stable air, such as the stratosphere, upward motion ceases. As a result, the air from the updraft diverges horizontally, depicted in Figure 7. Doppler radar measurements of storm-top horizontal divergence was first explored by Snapp (1979) and further explored by Lemon and Burgess (1980), who concluded that the use of storm-top divergence can be useful in real-time warning operations as it is a good indicator of updraft strength.

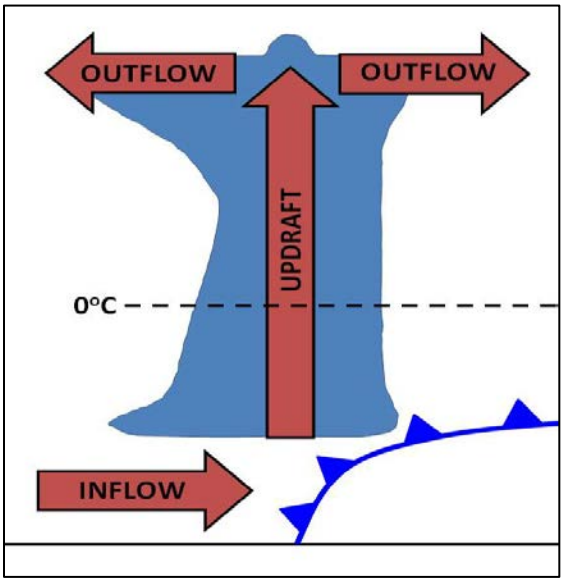

Figure 7. Basic thunderstorm flow structure. Updraft termination results in horizontal divergence or outflow.

The freezing level is defined as the altitude at which the air temperature first drops below freezing (http://www.nws.noaa.gov/glossary, June 2009). The height of the freezing level is important because hail embryos must have sufficient time in a cloudy, subfreezing environment to grow by accretion into large hail (Ziegler 1983). Melting has a lower effect on hail size with lower freezing level heights while the effects of melting are increased with a much higher freezing level (Donavon 2007).

The wet-bulb zero temperature is the lowest temperature that can be obtained by evaporating water into air. The wet-bulb zero height is the height where the wet-bulb

temperature drops below freezing (see http://www.nws.noaa.gov/glossary, June 2009). The wet-bulb zero height may better correlate to hail size than the freezing level as the height of the freezing level, observed at 12 UTC and 00 UTC, will likely decrease to the wet-bulb zero height as convection pumps low-level moisture into the upper levels of the troposphere.

In 1951, Fawbush and Miller stated that for air to be convectively unstable a shallow moist layer of air is needed at the surface and a deep layer of dry air must be in place aloft. Thunderstorms in the mid-latitudes are made stronger by dry mid-levels as dry air is denser than moist air. When an updraft pumps warm moist air from the surface into the mid-levels of the atmosphere where the conditions are cool and dry, the large density differences between the updraft and the surrounding atmosphere cause for explosive updraft development. Falling precipitation from the thunderstorm will evaporate into the surrounding dry atmosphere, a process that absorbs latent heat, effectively lowering the height of the freezing level. The pre-convective wet-bulb zero height may indicate the height of the freezing level after convection has developed.

D. MAXIMUM STORM-TOP DIVERGENCE AND THE FREEZING LEVEL

Boustead (2008) correlated both max storm-top divergence and the freezing level to forecast hail size. In his research, Boustead interrogated 100 thunderstorms, 62 were supercells and 38 were multicells. He also limited his research to storms that occurred in the Northern and Central Plains of the United States. The geographical boundaries used by Boustead for storm selection are depicted in Figure 8.

Boustead found that storm-top divergence correlated with hail size such that larger values of storm-top divergence produced larger hail. Consequently storm-top divergence was found to have utility in an operational warning environment for hail size prediction. The inclusion of freezing level data increased the correlation between storm-top divergence and maximum hail size. Using his results, Boustead produced a forecast table which, given the height of the freezing level, provides a forecast hail size based on the observed storm-top divergence from the thunderstorm in question.

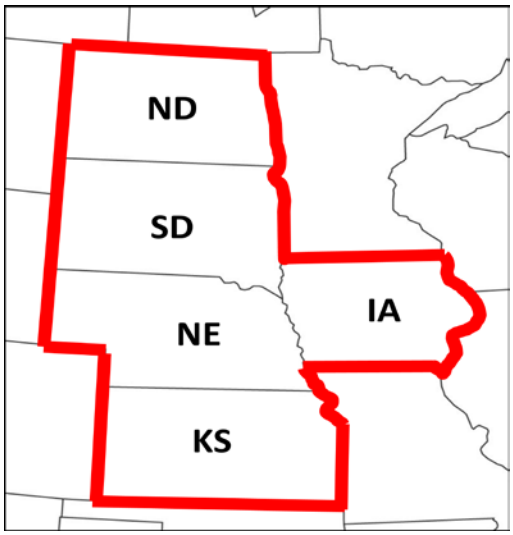

Figure 8. Northern and Central Plains of the United States. The boundaries outlined by Boustead (2008) include North and South Dakota, Iowa, Kansas, and Nebraska.

Weather forecasters from the 15 OWS actively utilize Boustead's forecast table for interrogating thunderstorms and forecasting maximum hail size. And while the table proves useful in the Northern and Central Plains, the hail forecast table tends to over forecast hail size in the Northeastern U.S., including the New England and Mid-Atlantic States regions. Even though the supercell is the rarest of storm types, they occur with a higher frequency over the Great Plains than anywhere else in the United States and were the primary storm type in Boustead's study. Although supercells do occur over the Northeastern U.S., they are vastly outnumbered by the other thunderstorm types and may account for hail size over-prediction when applied to this region. Since Boustead investigated both supercells and multicells without distinction, further research must be accomplished by separating supercells from the other thunderstorm types.

As previously stated, supercells are dynamically different from multicell and single-cell thunderstorms. The duration of the single cell within a supercell is on the order of hours while the duration of a single cell within a single-cell or multicell storm is typically 30 minutes to an hour. While updraft strength determined from storm-top divergence correlates to maximum hail size, updraft duration also plays a role in overall

hail size as short lived cells—no matter how strong—cannot develop large hail due to lack of time. The goal of this research is to look specifically at non-supercell storms to determine if the amount of storm-top divergence observed correlates to a different range of hail sizes than that of the supercell convection documented by Boustead (2008).

THIS PAGE INTENTIONALLY LEFT BLANK

III. METHODS AND PROCEDURES

For this research, nine synoptic scale events were chosen having produced numerous hail reports over the Northeastern U.S., the region where Boustead's hail forecast table is likely to be less effective. Because this research is focused on studying non-supercell thunderstorms, these nine events were selected with the expectation of having a small amount of supercells. Radar data was analyzed to obtain storm-top divergence values and determine storm type. Other synoptic data was gathered for each storm to include surface temperature and dew point, freezing level height, and the wet-bulb zero height. The methods and procedures involved in this research are listed below.

A. SYNOPTIC EVENT SELECTION

In picking the synoptic events for this study, it was important to limit the amount of supercell thunderstorms cases to ensure the maximum amount of non-supercell thunderstorms for analysis. Utilizing the Storm Prediction Center's (SPC) database of storm reports, specific dates were chosen where numerous hail events were reported over both New England and the Mid-Atlantic States regions with relatively few tornado reports over the same areas (see http://spc.noaa.gov/climo/reports/). Figure 9 depicts the storm report geographical distribution for one of the events utilized in this study.

The monthly and annual summary page from SPC, which can be found within the storm reports page, organizes storm report data annually and includes a list of "Top Ten Active Days" for each year. From this page, nine dates were selected with a high amount of hail reports and a lack of tornado reports over the Northeastern U.S., ranging from 2007 through 2011. Next, these dates were entered into the "Past Storm Reports" page, producing a list of all the storm reports from that date, separated into Hail, Damaging Winds, and Tornadoes. Each hail storm report includes, but is not limited to, the time of the report, size of the hail in inches, and the geographical coordinates of the report. A small example of an SPC storm report list is shown in Figure 10.

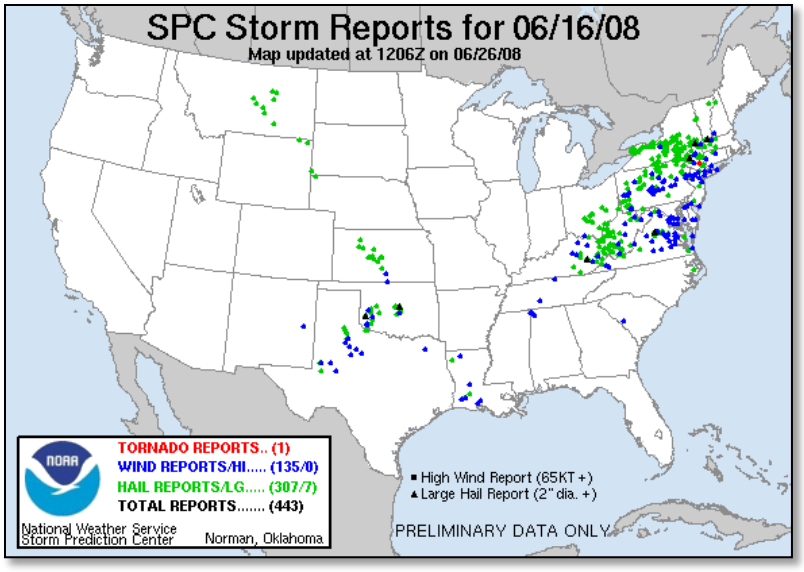

Figure 9. Sample SPC storm report map from 6 Jun 2008, covering 6 Jun 2008/ 12 UTC to 7 Jun 2008/ 12 UTC. The blue dots indicate damaging wind reports, the green dots indicate large hail reports, and the red dot indicates a tornado report.
(Image from http://www.spc.noaa.gov/climo/online/).

Hail Reports (in CSV format)

Time	Size	Location	County	State	Lat	Lon	Comments
1640	88	DINGMANS FERRY	PIKE	PA	4122	7488	(BGM)
1655	88	5 W ELDON	WAPELLO	IA	4092	9232	(DMX)
1715	75	FAIRFAX	CITY OF FAIRFAX	VA	3885	7730	PENNY SIZE HAIL REPORTED AR FAIRFAX CIRCLE AND AT PROPERTY YARD IN THE CITY OF FAIRFAX. (LWX)
1822	75	MOUNT CARROLL	CARROLL	IL	4210	8998	AND VERY HEAVY RAIN (DVN)

Figure 10. Sample SPC storm report list from 27 Jun 2007, covering 27 Jun 2008/ 16 UTC to 19 UTC. The first and third reports fall within the geographical boundaries of the study.
(Image from http://www.spc.noaa.gov/climo/online/).

The list of reports can also be exported into a Microsoft Excel spreadsheet, which was utilized to store and manipulate other collected data from this research. Accepted storm reports for the study were limited to the New England and Mid-Atlantic States

regions. The following 11 states from which the reports were filtered are: Connecticut, Delaware, Maine, Maryland, Massachusetts, New Hampshire, New Jersey, New York, Pennsylvania, Vermont, and Virginia. Storms that occurred within the listed states but west of the Appalachian Mountains were omitted from the study as they occurred outside of what is considered the Mid-Atlantic States region. The outline of the geographical region is shown in Figure 11.

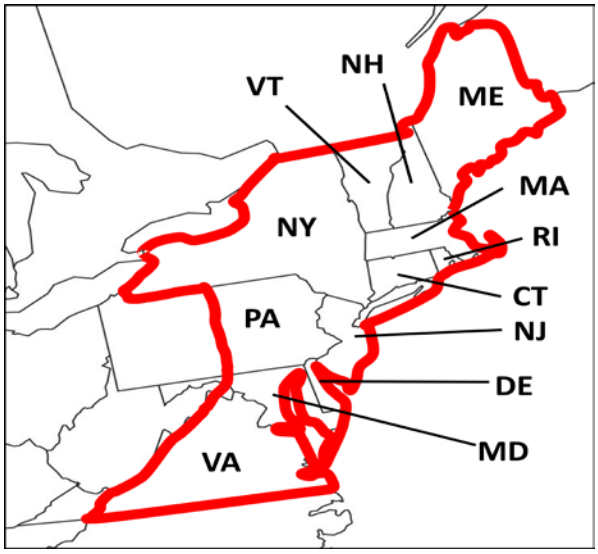

Figure 11. Northeastern U.S. and the Mid-Atlantic States region. The states for thunderstorm analysis used in this study include Connecticut, Delaware, Maine, Maryland, Massachusetts, New Hampshire, New Jersey, New York, Eastern Pennsylvania, Rhode Island, Vermont, and Virginia.

B. RADAR DATA

Once the excel spreadsheets of severe hail reports for each synoptic event were compiled, the next step was to identify the nearest Doppler radar site, which was accomplished using Google Earth. Historical radar data was acquired from the National Climatic Data Center (NCDC), which maintains archived Level II and partial Level III data from the past few decades (see http://www.ncdc.noaa.gov/nexradinv/). Radar data was used to determine storm-top divergence and the thunderstorm type.

For this study, Level II radar data was used because the Level III data did not include elevation scans higher than 3.4 degrees. Higher elevation angles, up to 19.5 degrees, were required to interrogate the majority of the thunderstorm tops from this study as the lower elevation scans penetrated the lower or middle portions of the storm. While storm relative velocity products of Level III radar data are extremely useful to operational forecasters when interrogating real-time storm data, the available Level II base data fulfilled the needs of this study as storm top divergence can be calculated without compensating for the motion of the storm (Figure 12).

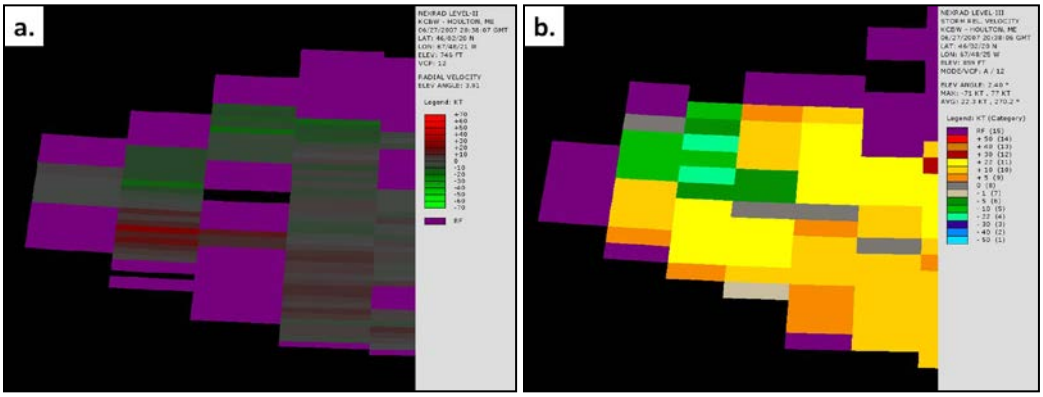

Figure 12. Velocity return of a thunderstorm from 27 June 2007 at 2038 UTC. Doppler radar (a) Level II Radial Velocity and (b) Level III Storm Rel. Velocity. Note: The radar site is located north of the echo where up is north.

On the other hand, Velocity Folding became an issue due to use of Level II data, as the resulting false data is only fixed by algorithms in Level III data. Doppler radar can determine flow speed if it is moving toward or away from the radar. The radar sends a pulse out toward precipitation masses at a specific wavelength. The phase of the returning pulse will differ from the phase of the initial wavelength if the precipitation is moving toward or away from the radar. By comparing the initial and final wavelength phase differences, the radar determines the inbound/outbound direction and speed of the flow. When flow speed becomes great, the resulting phase shift can be larger than the initial wavelength itself, which would then appear as a small phase shift from the initial wavelength in the opposite direction. An example of this would occur when the majority

of the flow is moving away from the radar, but the center of the flow depicts strong inbound values. In reality, this area of inbound flow would actually be the strongest outbound flow.

In the example depicted in Figure 13, a thunderstorm is depicted by both the base reflectivity scan in Figure 13.a and the radial velocity scan in Figure 13.b. With respect to the radar, red values on the velocity scan indicate outbound winds while green values indicate inbound winds. The strongest reflectivity return in Figure 13.a was transposed to the velocity scan to indicate the center of the thunderstorm—see the orange square in Figure 13.b. This particular storm was discarded because the radial velocity pattern depicts convergence at the top of the storm instead of divergence, as green inbound values to the left of the storm center meet red outbound values to the right of the storm center. Since divergence is expected at the top of a thunderstorm, the converging winds depicted can be attributed Velocity Folding since the inbound and outbound values include no real transition where one is expected. The storm from this example, like many others in this research, was discarded.

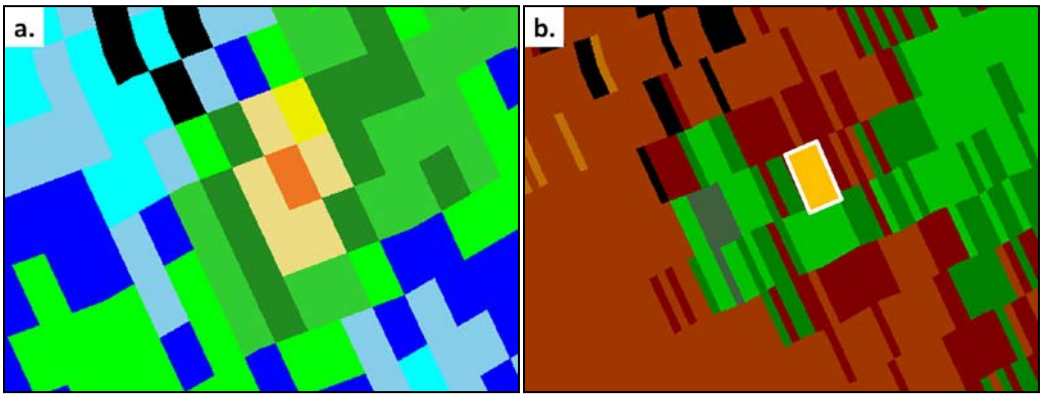

Figure 13. Radar return of the top of a thunderstorm from 16 June 2008 at 1840 UTC. The maximum reflectivity value from the (a) reflectivity scan was transposed to the (b) radial velocity radar scan. Note: The radar is located to the northeast of the storm, which is to the top right of the image.

Boustead (2008) interrogated every radar scan from 15 minutes prior to the storm report up to five minutes after in hopes of measuring the maximum storm top divergence produced by the hail producing cell. A different method was used in this research to allow for a larger sample size as more than 400 storms were analyzed, reducing the time spent analyzing each storm. Instead of examining multiple radar scans, only one radar scan was surveyed, selected between five and ten minutes prior to the storm report time. In addition, since all of the thunderstorms interrogated in this research have multiple cells, identifying the cell that produced the hail in the report was occasionally problematic, especially for the multicell storms that encompass multiple short-lived cells. Viewing multiple radar scans in attempt to retrieve the maximum storm-top divergence might be futile as the max divergence may have been observed in a cell that did not produce the reported hail.

1. Storm Identification Issues

The IDV software was used to display the radar files and to plot the geographical location of the storm report. In certain cases, the storm report was in close proximity to the only storm in the vicinity. In other situations, the storm report location would appear in the middle of a cluster of thunderstorms, making it difficult to pick the correct parent storm. During these instances, an educated guess was used to select the correct storm with the knowledge of the synoptic conditions, i.e., knowing the direction of the upper-level winds in hopes that hail would have come from that direction. If the

Another issue that surfaced during analysis was that some reported storm locations were far away from the nearest radar echo based on the time of the report. See the example depicted in Figure 14. Cases such as this can be attributed to error in hail report times, a delay in reporting the event, or incorrectly reporting the storm location. Hail events such as this were discarded from the study as storm measurements could not be used without knowing why the hail reported location or time was far removed from the storm itself.

The last prevalent issue within this research was the result of dealing with multicell storms or a large cluster of multicell storms. The short lived nature of an individual cell within a multicell storm occasionally made it difficult to determine which

cell was responsible for the reported hail. The hail report could have been relayed a considerable time after the hail actually fell. Thus the cell that actually produced the hailstones may have collapsed and not been evident on the scan that was analyzed.

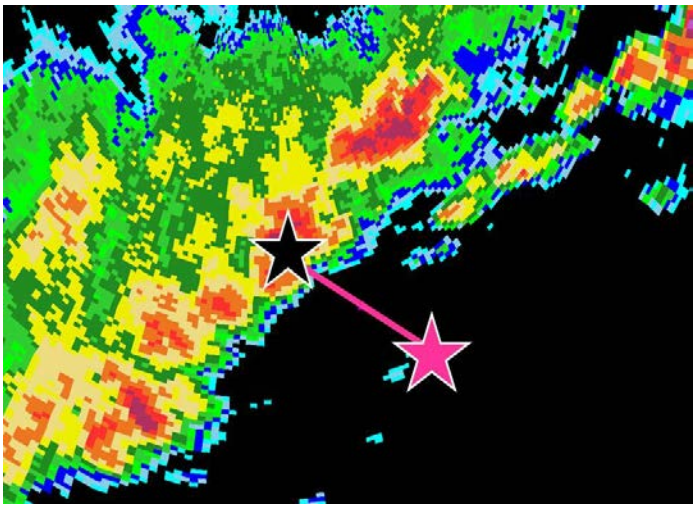

Figure 14. Radar reflectivity scan on 16 Jun 2008 at 2025 UTC. The pink star indicates a hail report at 2030 UTC. The nearest thunderstorm echo is indicated by the black star, which is over 40km from the hail report location.

2. Storm-Top Divergence

The IDV software was used to view the radar files from NCDC (see http://www.unidata.ucar.edu/software/idv/). After the radar data was plotted, a geographical coordinate marker was placed at the location of the storm report to aid in identifying the originating thunderstorm. Velocity values were rounded to the nearest knot and entered into the excel spreadsheet from SPC. If an elevation scan greater than 10 degrees was required to view the top of the thunderstorm, a combination of two elevation scans were used to measure the storm-top divergence. Inbound velocity values toward the radar were obtained using the highest possible elevation scan while outbound velocity values were obtained using the next lower scan. This adjustment was made to compensate for the possibility that the highest elevation scan penetrated the inbound half of the storm top while overshooting the outbound half, an example of which is depicted in the Figure 15 illustration.

Normally, the unit for divergence is in meters per second (ms^{-1}). However, Boustead (2008) used knots instead of ms^{-1} since knots are widely used by operational meteorologists to describe wind speed. The issue that arises from the use of knots is that the distance between the maximum inbound and outbound values is not taken into account. As the distance between the measured flow increases for a specific inbound/outbound couplet, the representative updraft strength becomes weaker. The storm-top divergence values will be less representative of the updraft strength when the distance within the inbound/outbound couplet is great. However, this is an issue that cannot be avoided in the operational environment when interrogating the top of a thunderstorm. Additionally, the average error should be reduced by a large sample size.

3. RADAR ERRORS

Other issues that appeared within this study occurred due to the limitations of the WSR-88D system. The radar scans multiple elevations with the purpose of producing a detailed picture of the thunderstorm. The lowest elevation scan is transmitted at a 0.5 degree angle above the Earth's surface while the highest elevation scan, when set to a convective volume coverage pattern, is 19.5 degrees above the Earth's surface. If the thunderstorm is too close to the radar, then the 19.5-degree scan will pass through the middle of the storm and the top of the storm will not be sampled. Thus thunderstorms too close to the radar had to be discarded from the study.

As radar pulses travel away from the radar, the vertical distance between the subsequent pulses increases. Because of this, storms that lie far away from the radar are less likely to have the top of the storm interrogated. For example, if a radar pulse passes through the upper-portion of a thunderstorm, it will likely measure horizontal divergence but might not capture the strongest divergence located at the top of the storm. If the next pulse passes above the storm top, then the max storm-top divergence is not measured. For an illustrated example, see Figure 16. This leads to uncertainty in the storm-top divergence that could not be eliminated. By keeping the sample size large, the statistical mean should be useful as there is no reason to expect systematic error in the storm-top

divergence measurement. In addition, to apply this in operation, the same uncertainty exists and tools that include any bias will be directly applicable.

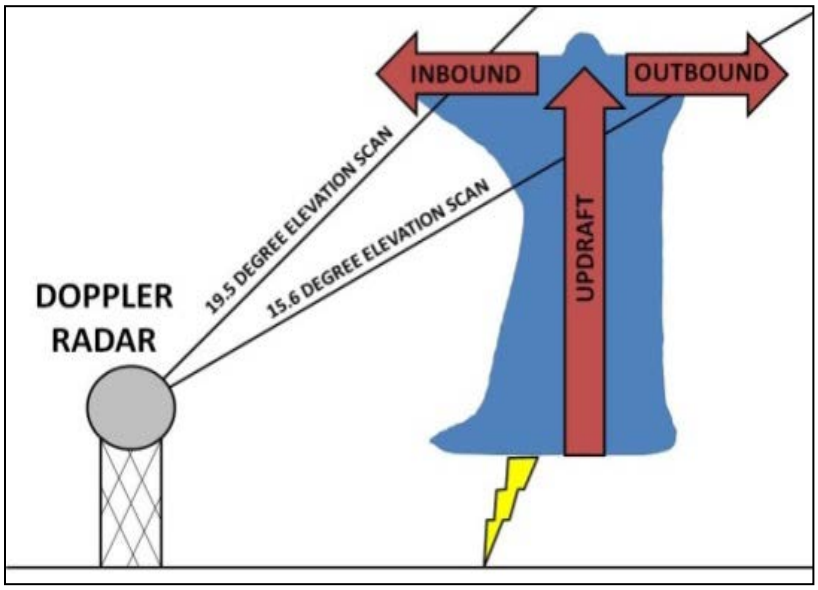

Figure 15. Illustration of a thunderstorm in close proximity to a Doppler radar site. Radar elevation scans leaving the radar dome penetrate the thunderstorm in different places, each measuring different halves of the storm-top. Note: Illustration is not to scale

Next, Range Folding is an issue when a thunderstorm is located beyond the extent of the radar range, which can cause echoes to appear within the range where no echo is actually present. Weather radar works by sending out a radio pulse which is reflected off of precipitation. The radar then measures the reflected energy and this data is then used to display a graphical depiction of the precipitation. If returned energy from an old pulse, reflected off distant precipitation, returns at the same time as energy returns from the current pulse off of closer precipitation, the data is then compromised as the radar will show one area of precipitation because it cannot distinguish between the pulses to know that they came from different distances from the radar. If range folding obstructed the target storm, then the storm was discarded from the study. Additionally, if a subsequent radio pulse is transmitted before the original pulse is reflected and returns to the radar, the radar views this original energy as a coming from the subsequent pulse. Thus the

returned energy, which came from a considerable distance from the radar appears to have come from a close distance and is therefore not representative of the real atmosphere.

Lastly, a few storms were discarded due to radar maintenance. If a storm report could only be interrogated by one radar site and that site did not have data for the time of storm, it was assumed that the radar was logged out for maintenance and was waiting for repairs to be completed before returning to service. In these cases, hours of data were missing from the NCDC radar files and thus storm analysis was impossible.

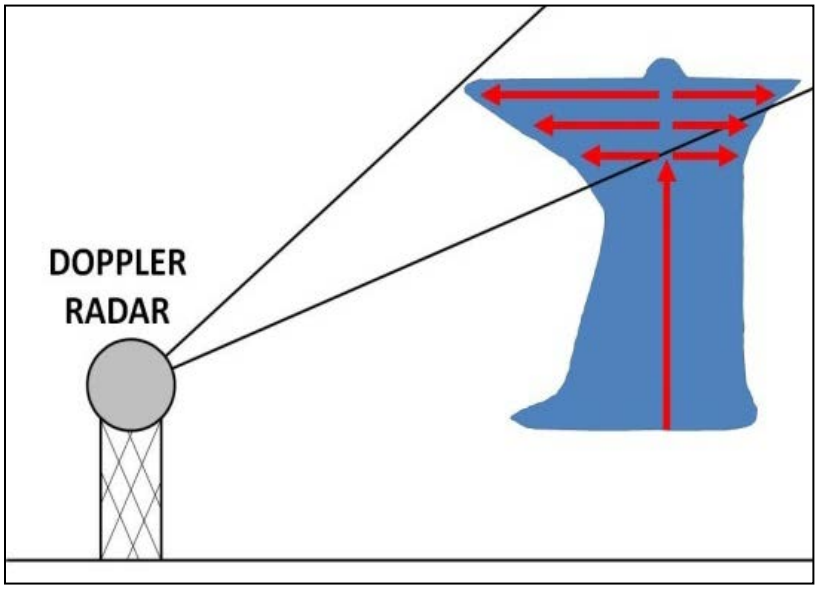

Figure 16. Illustration of a thunderstorm where radar scans do not pass through the region of strongest storm-top divergence. The vertical distance between radar scans increases with distance from the radar. Divergence is depicted by the horizontal arrows within the upper half of the thunderstorm. Longer arrows indicate higher wind values. Note: Illustration is not to scale.

4. Storm Type

Next the storm type was identified and cataloged. Storms were categorized into three types; Bow Echoes, Multicells, and Squall Lines. Instances of Quasi-Stationary mesoscale convective systems, or training thunderstorms, were observed. However, the individual thunderstorms within the training thunderstorms were either classified as

multicells or supercells. If a supercell was identified by the presence of strong rotation throughout the vertical structure of the thunderstorm, no further interrogation and data collection was conducted.

C. THERMODYNAMIC INFORMATION

Storm-top divergence alone may not be the best indicator of the resulting hail size as other factors play a key role in hail development and sustainment. The other observed meteorological data compiled for each storm case were the surface temperature and dew point, height of the freezing level, and the wet-bulb zero height.

1. Surface Temperature and Dew Point

Both Google Earth and a meteorological tool from the Aviation Digital Data Service's (ADDS) were utilized to obtain surface temperature and dew point information near the reported hail position. The geographical location of the storm report was plotted in Google Earth, then matched against the network of surface observations as depicted by the ADDS METARs Java Tool (see http://aviationweather.gov/adds/metars/java/).

Once the nearest observation site was identified, the station identifier was entered into the USAF's 14th Weather Squadron climatology page to obtain historical surface observations (https://notus2.afccc.af.mil/SCIS/). The most recent observation reported prior to the storm report was used to supply the temperature and dew point. However, on numerous occasions, observations were either not available or did not include the temperature and dew point in the report. In these instances, the next nearest observation location was selected for the data set.

The surface observation network in the United States is fairly dense with numerous observations, especially some states over others. However, the density is still low enough that hail event locations were numerous miles away from an observation station. While the observation report should be fairly representative of the surface conditions at the location of the storm, geographical differences in the terrain could cause substantial differences. For example, if the storm occurred at the base of a mountain and the nearest observation was located halfway up the mountain, or the observation location is next to a river while the storm is upstream from the river, then the temperature and dew

point data of the observation may differ greatly from what was present at the location of the storm. In addition, when the nearest observation could not be used and the next nearest station was utilized, uncertainty introduced by their lack of spatial collocation cannot be eliminated, but it is assumed that with a sufficiently large sample of events, these errors will average out.

2. Freezing Level and Wet-Bulb Zero

Boustead utilized NCEP's Rapid Update Cycle model for real-time vertical atmospheric profiles. However, this data is not easily obtainable after the subsequent model run. Alternatively, observed soundings, were used to provide both the freezing level and wet-bulb zero heights. These soundings are normally released every 12 hours at 00 UTC and 12 UTC. Both the height of the freezing level and the wet-bulb zero heights were taken from the preceding sounding unless the storm report occurred within three hours of the following sounding. This step was employed to minimize the affect of convection altering the freezing level and wet-bulb zero heights while trying to ensure the most representative values were used.

Sounding proximity was used to determine the most representative atmospheric conditions for the thunderstorm that produced the reported hail. Using the same method to determine the closet radar to the storm report, all of the upper air sounding sites were plotted in Google Earth, enabling the closest sounding site to be selected after plotting each hail report. Historical soundings and text data were retrieved from the Plymouth State Weather Center Archived Data page (http://vortex.plymouth.edu/raob_conus-u.html). As with the observations, some sounding data were not available for the requested time, thus the next nearest sounding site was utilized.

The upper-air sounding network over the United States is much less dense than the surface observation network. Many states only have one sounding while some have two. As a result, the nearest sounding location was often hundreds of miles away from the hail event location. This distance was further lengthened in the event that sounding data was missing and another sounding had to be used. Such large distances from the sounding location to the hail event location could lead to large differences in atmospheric

conditions at the location of the sounding and at the location of the hail event. Presumably consistent larger scale environmental structure helps mitigate some of this distance error and as with other observational error, the large sample size will reduce the average error.

Additionally, as soundings are only conducted twice a day, changes to the atmospheric profile are probable. The atmospheric representation for the hail events that were reported between soundings was likely less accurate. However, this is the reason for including the wet-bulb zero height in this study, which should be less impacted by evolution of the atmosphere through the day in the presence of convection.

THIS PAGE INTENTIONALLY LEFT BLANK

IV. RESULTS

During this research, 412 storms were selected for radar analysis. Through radar interrogation, 104 storms were either rejected or identified as supercells due to the presence of strong low-level or mid-level rotation on the radial velocity scans. The remaining 308 storms were identified as non-supercells. The remaining 64 storms were rejected for various reasons as listed in the previous chapter, including missing radar data, echo proximity to the radar, or the hail report location and time not lining up with the radar scan.

As a result, additional data for the 308 non-supercells were compiled and statistically analyzed. Moreover, the storms were separated into three thunderstorm categories; bow echoes, multicells, and squall-lines; no single-cell storms were observed. Data compiled and manipulated for each storm include reported hail size, measured storm-top divergence, and observed temperature, dew point, freezing level, and wet-bulb zero height. The following section first compares the non-supercell storm types, breaking down the differences between the observed storm types and their observed storm-top divergences. Next, the hail size statistics are compared to the reported hail sizes of the supercells rejected by this study. Subsequently the individual parameters are compared, looking for correlations to hail size and storm-top divergence. Lastly, the life cycle of a hail producing cell within a multicell storm is examined.

A. NON-SUPERCELL STORM TYPES

The vast majority of the 308 storms were categorized as multicells, totaling 243. Squall-lines were the next most observed with 57 cases identified. Lastly, eight storms were categorized as bow echoes. This distribution is shown in Figure 17.a. Additionally, the average hail size recorded by multicells, shown in Figure 17.b, was lower than that of the average hail sizes of both the bow echoes and squall lines cases. The larger hail sizes from squall-line thunderstorms directly correlate to the stronger measured storm-top divergence values as shown in Figure 17.c. Lastly, the average surface dew point, show in Figure 17.d, was 2 degrees lower for the multicells than squall-lines, which infers

weaker atmospheric instability present to drive the updraft strength of the thunderstorms. Contrarily, the average surface temperature of multicells was 1 degree higher than for squall lines.

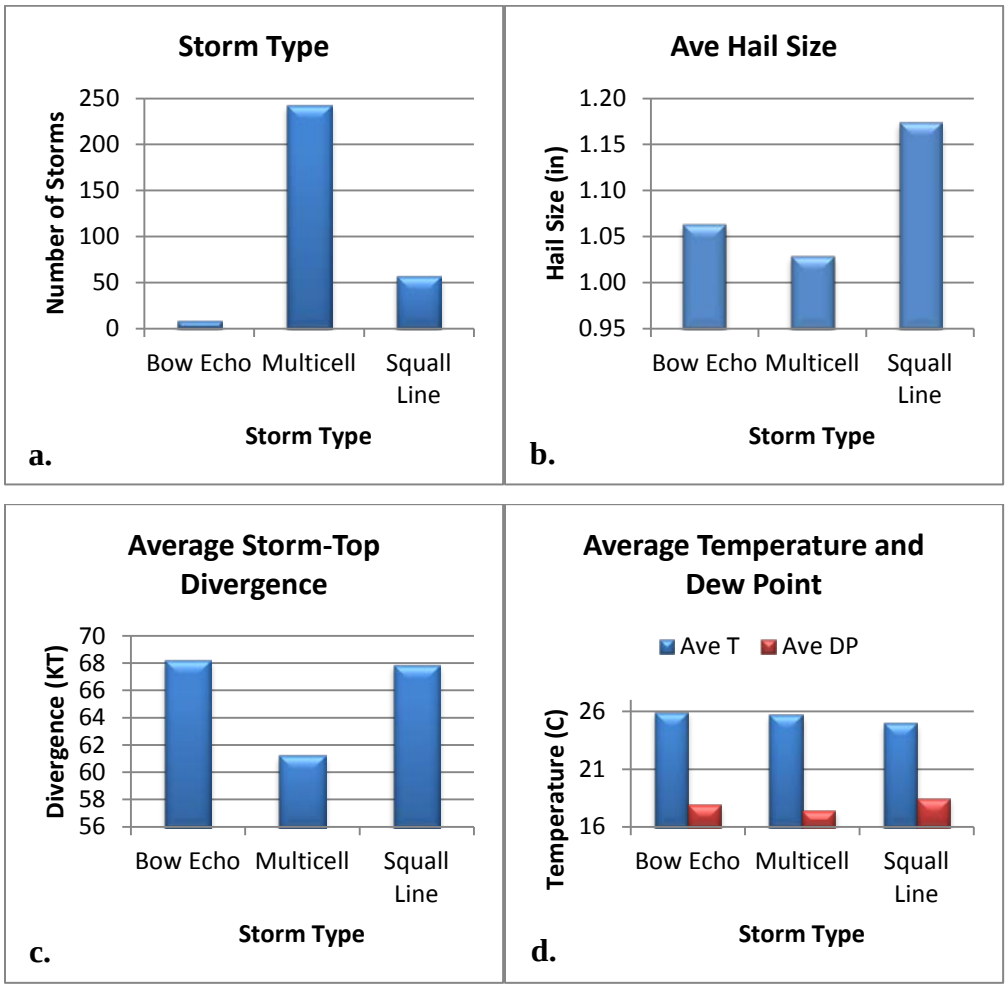

Figure 17. Distribution of storm types based on their (a) total count and the average (b) hail size, (c) storm-top divergence, and (d) temperature and dew point.

B. SUPERCELL AND NON-SUPERCELL THUNDERSTORMS

An initial comparison of the hail size distribution was made between all 308 non-supercell thunderstorms and the 60 supercells identified in this study. Further comparisons between multicell and squall-line thunderstorm hail sizes were conducted within the non-supercell category.

A breakdown of the 308 non-supercell hail reports revealed that 73% of the reported hailstones were 1.0 inch or less while hailstones 1.5 inches or greater accounted for 19% of the reports. In contrast, hailstones 1.5 inches or greater accounted for 32.5% of the supercell hail reports. Additionally, 2.0 inch or greater hail accounted for just over 2% of non-supercell hail reports while accounting for 12.5% of reports from supercells. See Table 1 for a complete percentage distribution.

Hail Size (in)	Non-Supercell	Supercell	Multicell	Squall-Line
0.75	24.4%	12.5%	25.9%	19.3%
0.88	27.3%	17.5%	27.6%	26.3%
1.00	21.8%	37.5%	23.1%	14.0%
1.25	7.8%	0.0%	8.2%	5.3%
1.50	8.1%	2.5%	5.8%	19.3%
1.75	8.4%	17.5%	8.2%	8.8%
≥2.00	2.3%	12.5%	1.2%	7.0%

Table 1. Hail size percentage of total storm reports for all non-supercell thunderstorms, all supercell thunderstorms, only multicell thunderstorms, and only squall-line thunderstorms.

For non-supercell thunderstorms, a linear decrease of hail occurrences is evident when hail size increases, as depicted in Figure 18.a. On the other hand, it is more difficult to detect a pattern from the distribution of hail reports from supercells. It is clear however that supercells are more likely to produce severe hail at the large end of the spectrum than non-supercells. Multicell and squall-line thunderstorms, depicted in Figure 18.b and 18.c, individually indicate a decreasing size trend for hail occurrences, although small severe hail occurrences were a higher percentage of the multicell reports than they were for the squall line reports.

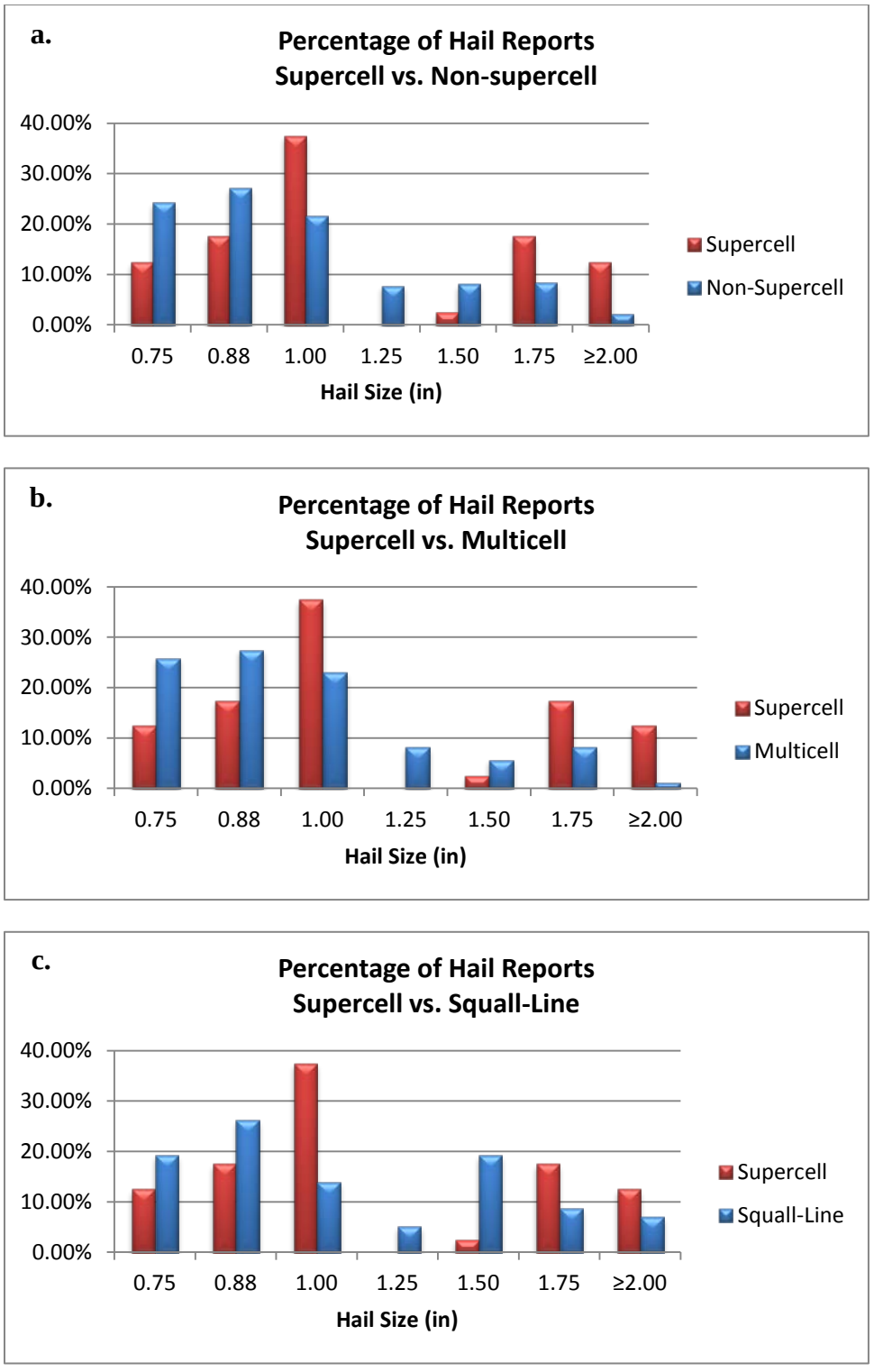

Figure 18. Percentage breakdown of total number of hail reports by hail size between (a) supercell and non-supercell hail reports, (b) supercell and multicell hail reports, and (c) supercells and squall-lines hail reports.

C. STORM-TOP DIVERGENCE

Boustead's hail forecast table begins with a minimum storm-top divergence value of 55KT and increased all the way to 231KT. However, of the 308 storms in this research, 112 or 37% had measured storm-top divergence values less than 55KT. Only 13 storms produced storm-top divergence values over 104KT with the maximum measured value being 130KT, thus the resulting scale for this study begins with lower values of storm-top divergence and does not peak as high as Boustead's. The distribution of storm-top divergence values produced by all non-supercell thunderstorms of this study is depicted in Figure 19.a. Figure 19.b indicates that the majority of the multicell storms produced values of storm-top divergence on the lower end of the spectrum. Figure 19.c shows that storm-top divergence values from squall-line thunderstorms were found in the middle of the spectrum and were more commonly stronger than multicells.

Storm-top divergence in 10 knot categories and their respective average hail size for all non-supercell thunderstorms are depicted in Figure 20.a. The average hail size increased as storm-top divergence increased, as evidenced by the plotted linear trend line. This trend is also evident for both multicell and squall-line hail reports, as shown by the plotted trend lines in Figure 20.b and 20.c respectively. However, sparse large hail reports skewed the average distribution, so box and whisker plots were utilized to remove the outlying bias of the occasional large hail report.

The box and whisker plot in Figure 21.a captures the storm-top divergence values for all non-supercell thunderstorms, which depicts the lower and upper quartiles and maximum and minimum occurrences of each hail size. The inner quartile range illustrates a distinctive increase in storm-top divergence measured as reported hailstone sizes increased without being influenced by the outlying maximum and minimum reports. The slope trend of the inner quartile is fairly linear, although the 1.5 inch category had a higher inner quartile range than the 1.75 and the ≥2.0 inch bins. Both multicells and squall-lines individually depict this increase, as depicted in Figure 21.b and 21.c. On the other hand, the larger hail bins become less linear, particularly for squall-lines, likely due to a small number of hail reports in the upper size range. Still, all three of these distributions support the concept that stronger storm-top divergences result in larger hail.

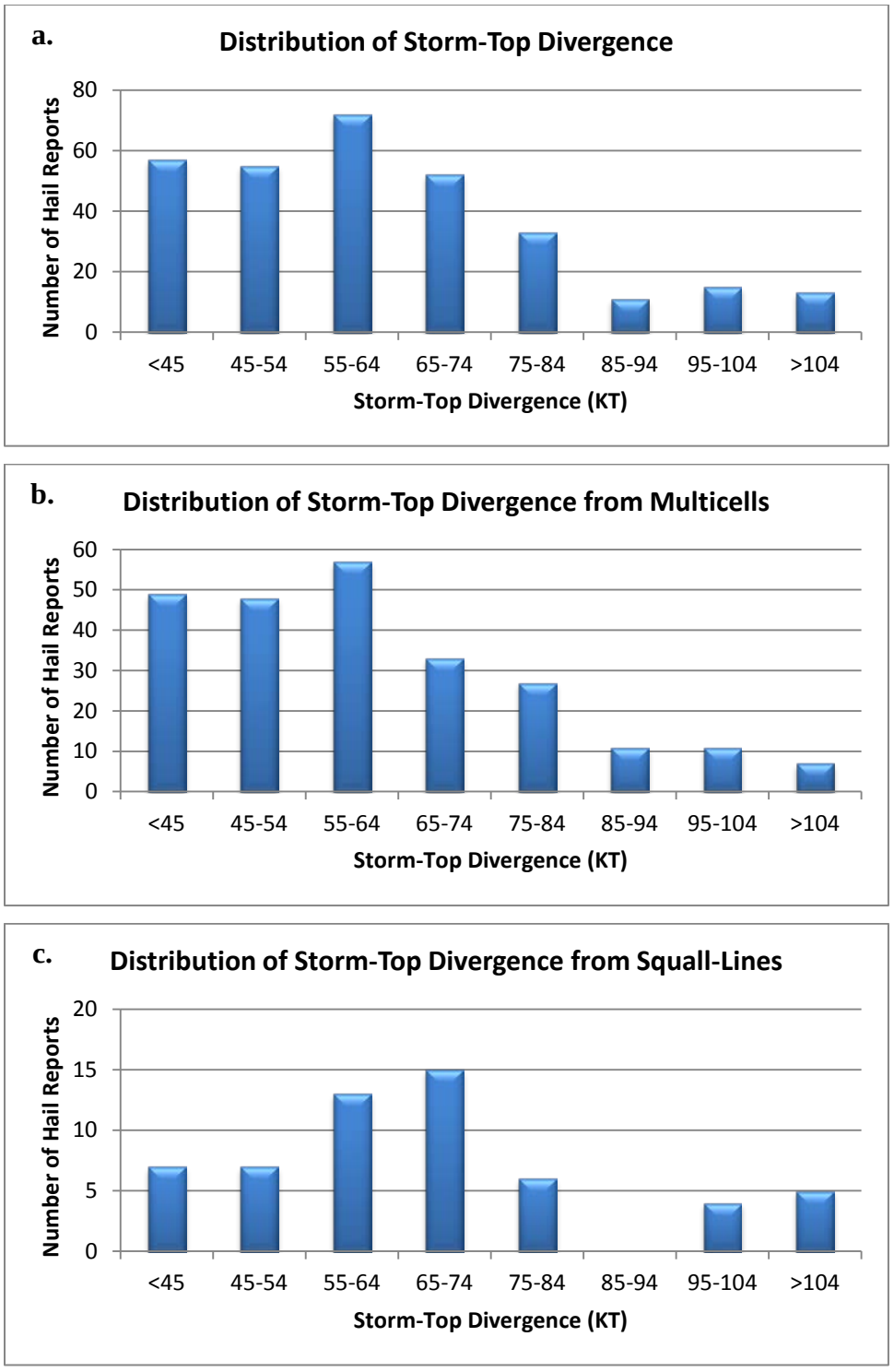

Figure 19. Distribution of storm-top divergence values measured from all (a) non-supercell thunderstorms and both (b) multicells and (c) squall-lines.

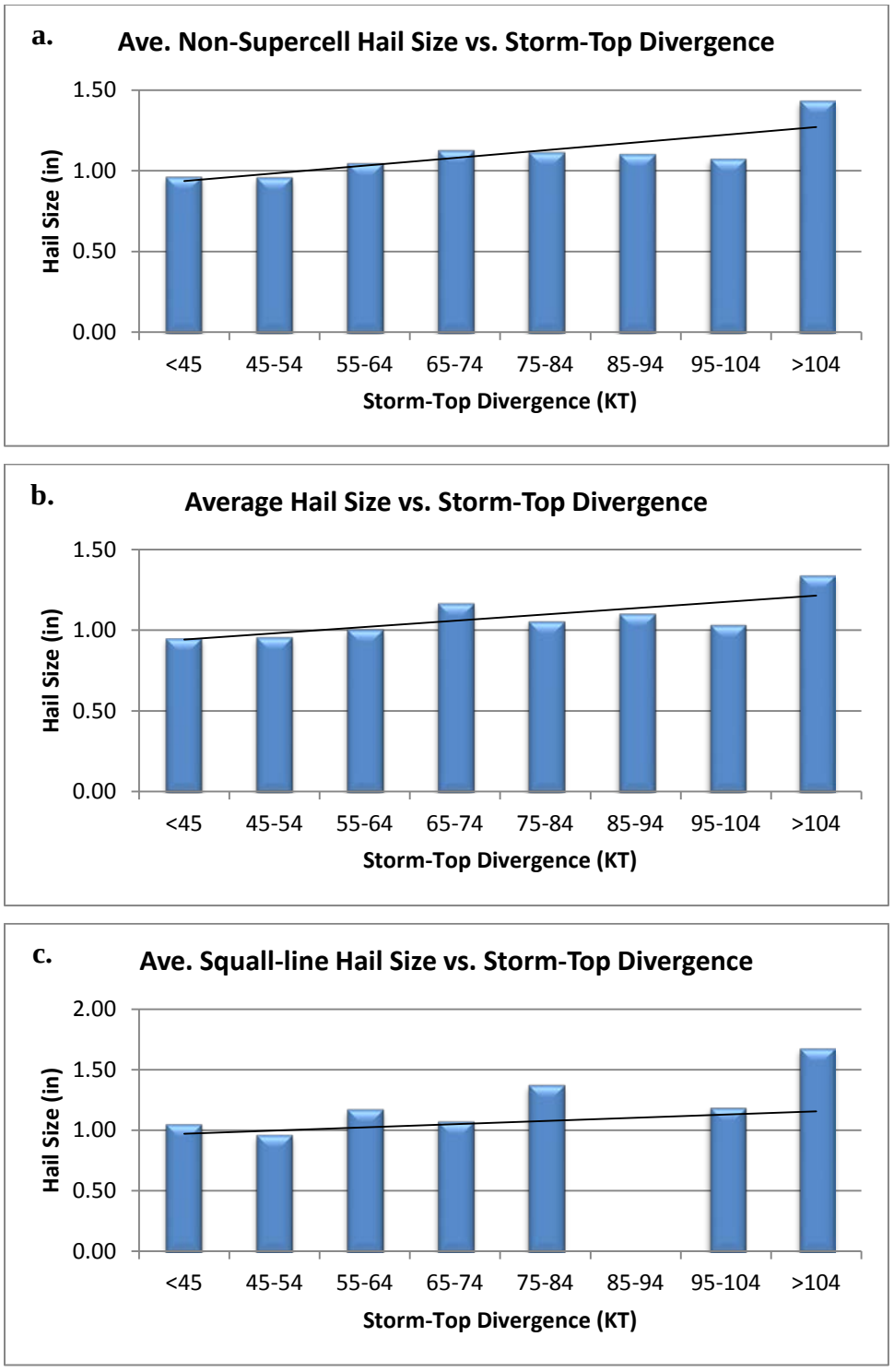

Figure 20. Histogram that separates the storm-top divergence values into separate categories and depicts the average hail size for (a) all non-supercells, (b) multicells, and (c) squall-lines. A linear trend line is depicted at the top of each chart.

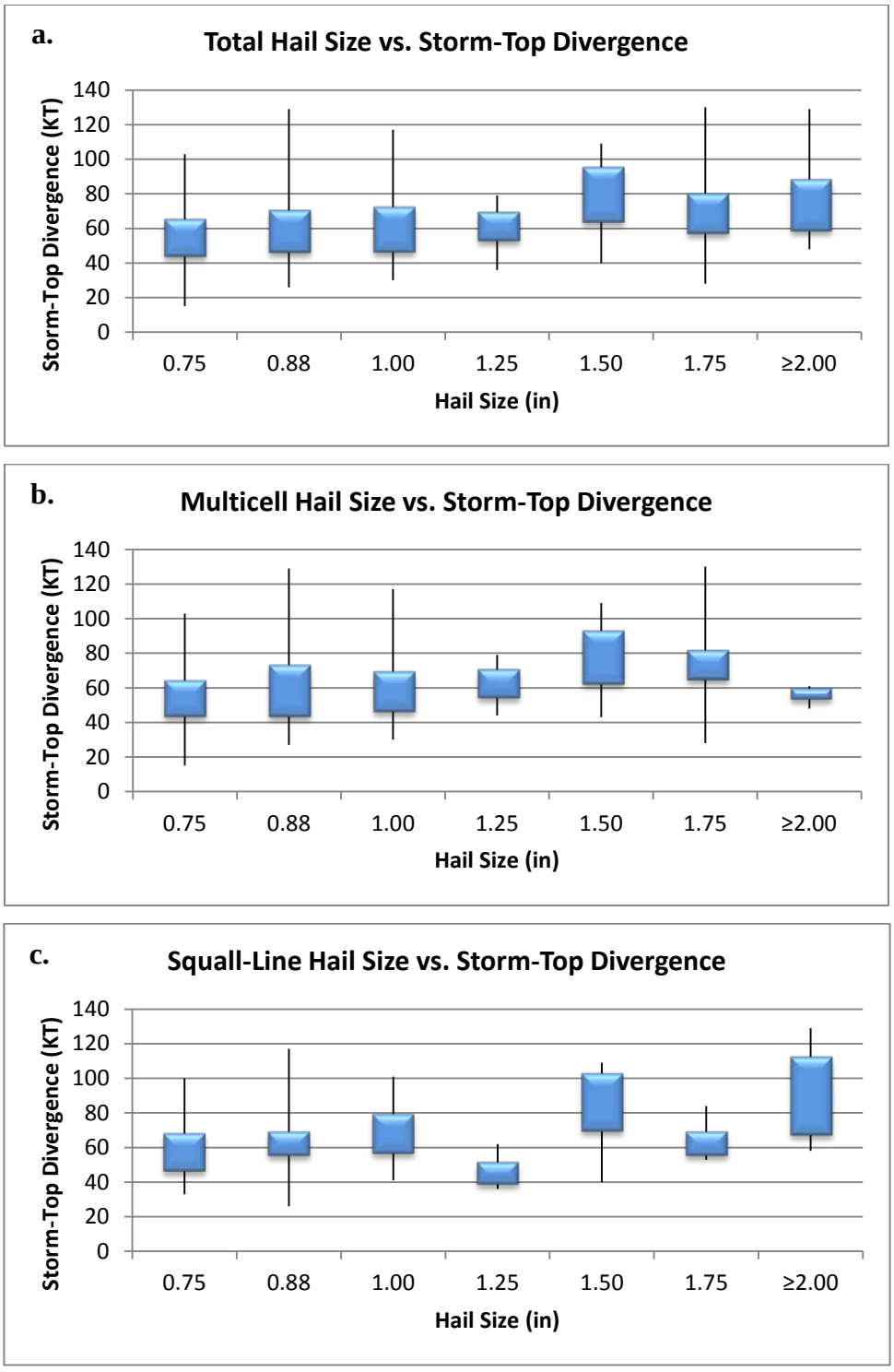

Figure 21. Box and whisker chart depicts storm-top divergence values for (a) all non-supercells, (b) multicells, and (c) squall-lines. Maximum and minimum values indicated by the vertical lines and inner quartile ranges represented by the boxes.

D. FREEZING LEVEL

To mimic the breakdown provided by Boustead, freezing level heights were separated into seven categories, two more than Boustead utilized. Without the two extra categories, the first and last categories would have contained a much larger number of hail reports than the others. The categories were distributed as follows; less than 9500 feet, 9500 to 10500 feet, 10500 to 11500 feet, 11500 to 12500 feet, 12500 to 13500 feet, 13500 to 14500 feet, and greater than 14500 feet. Table 2 includes the storm report distribution per freezing level category as well as the average storm-top divergence values and the average, maximum and minimum hail sizes.

Freezing Level (ft)	Number of Storms	Ave. Hail Size (in)	Max. Size (in)	Min. Size (in)
<9500	29	0.96	1.75	0.75
9500–10500	66	1.05	3.00	0.75
10500–11500	38	1.07	1.75	0.75
11500–12500	20	1.31	2.00	0.75
12500–13500	32	1.16	2.50	0.75
13500–14500	45	0.99	2.00	0.75
>14500	78	1.02	2.00	0.75
Total	308	1.06	3.00	0.75

Table 2. Distribution of freezing level heights and their respective number of storms and the average, maximum, and minimum hail sizes

From the data collected, it appears that a freezing level between 11500 and 12500 feet is more conducive for large hail than the other freezing level heights, given that other necessary convective conditions exist. However, the 11500–12500 category contains the smallest number of hail reports. Additionally, the maximum and minimum hail values for each category do not reveal much useful information. With the exception of the 9500–10500 and 11500–12500 categories, reports of 0.75 inches are numerous while large hail reports over 1.5 inches are scarce for all categories.

Table 3 displays additional data for each freezing level category, to include average storm-top divergence and average surface temperature and dew point. With the

exception of the 12500–13500 category, the storm-top divergence increased as the freezing level increased. The large storm-top divergence in the 12500–13500 category is likely due to a relatively small sample size within the category. The overall increase in storm-top divergence with freezing level height could be due to the fact that increasing freezing level heights infer increasing tropopause heights. The higher the height of the tropopause, the larger the vertical extent of the updraft within the thunderstorm, providing more time for vertical acceleration of air within the updraft, leading to increased storm-top divergence.

Freezing Level (ft)	Ave. Hail Size (in)	Ave. Storm-Top Divergence (KT)	Ave. Temp. (C)	Ave. Dew Point (C)
<9500	0.96	54	23	16
9500–10500	1.05	57	23	15
10500–11500	1.07	57	24	15
11500–12500	1.31	61	24	18
12500–13500	1.16	74	27	20
13500–14500	0.99	65	29	20
>14500	1.02	67	27	20
Total	1.06	63	26	18

Table 3. Distribution of freezing level heights and their respective average hail sizes, storm-top divergence, temperatures, and dew points.

As was done by Boustead (2008), scatter plots and trend lines were done by freezing level categories to highlight differences in the storm-top divergence and hail size based on varying freezing level heights. Figure 22.a through 22.g shows scatter plots of all the hail reports in each individual freezing level category. Figure 22.h is a scatter plot of all non-supercell hail reports for all freezing levels. Even though outliers are clearly visible in a few of the scatter plots, linear trend lines indicate that increased storm-top divergence results in larger hailstones. Although each freezing level yields a discernible linear trend, the overall magnitude of storm-top divergence tends to be less for lower freezing levels as seen in Table 3. To prove a correlation exists between both hail size and storm-top divergence and that the slope is truly positive, regression analysis was performed for each freezing level category, as well as all the combined reports.

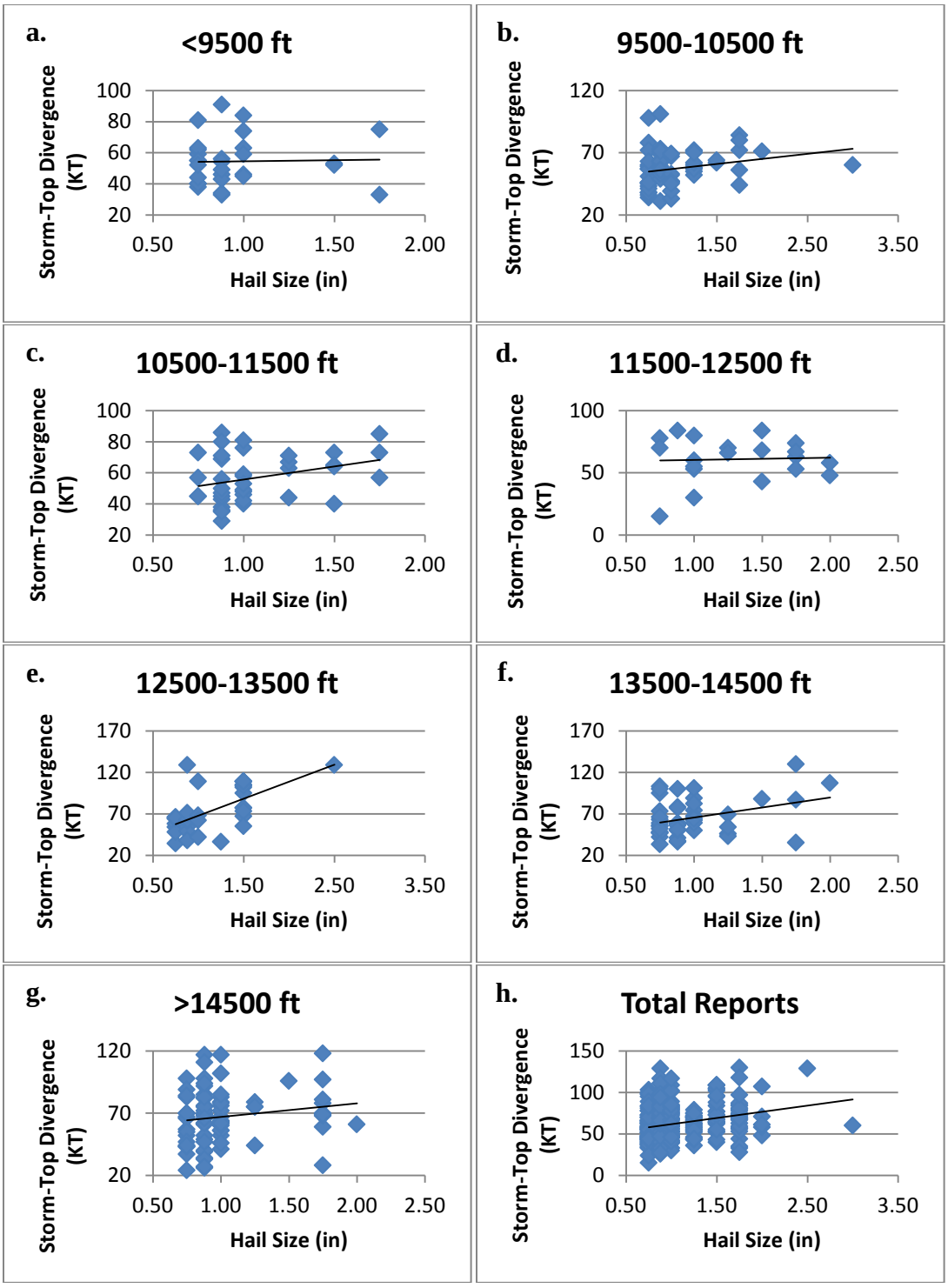

Figure 22. Scatter plots of each hailstone size with a linear trend line plotted. The plots are separated by freezing level in feet: (a) <9500, (b) 9500–10500, (c) 10500–11500, (d) 11500–12500, (e) 12500–13500, (f) 13500–14500, (g) greater than 14500, and (h) totals.

The regression analysis reveals that the overall slope between hail size and storm-top divergence is positive. The analysis also suggests that the slope is positive for each freezing level category, which coincides with the plotted linear trend lines from Figure 22. However, opposed to Boustead's findings, a few of the correlations between storm-top divergence and hail size derived from the slope within each freezing level category are not stronger than the correlation of all non-supercells. A 90% confidence interval test concluded that the slope is positive for total freezing level analysis as well as the individual freezing level categories of 9500-10500, 10500–11500, 12500–13500, and 13500–14500 feet. The slopes and confidence intervals are depicted in Table 4. This conclusion was reached because the confidence interval did not include zero or negative values. However, the confidence interval for the <9500, 11500–12500, and >14500 categories encompass zero and negative values, indicating that the possibility exists that the slope could be zero or negative. Thus there is uncertainty of the correlation surrounding these three individual freezing level ranges. The next step for the uncertain categories was to test the null hypothesis that the slope is either negative or zero.

Freezing Level (ft)	Number of Storms	Hail vs. Storm-Top Divergence Slope	Lower 90% Confidence Interval	Upper 90% Confidence Interval
<9500	29	1.44	-15.71	18.58
9500–10500	66	8.14	0.60	15.68
10500–11500	38	16.79	2.82	30.76
11500–12500	20	1.68	-15.21	18.57
12500–13500	32	41.12	24.51	57.73
13500–14500	45	24.21	6.74	41.68
>14500	78	11.04	-1.73	23.80
Total	308	14.93	9.67	20.19

Table 4. Slope and confidence interval statistics between hail size and storm-top divergence for each freezing level category.

The 90% confidence interval was also used for the null hypothesis test. Residual values for each storm-top divergence measurement were also analyzed, which is the difference between each observed and predicted storm-top divergence value based on the regression analysis. For null hypothesis testing, t-statistics and t-thresholds were

calculated from the regression results calculated in excel for the separate freezing level categories. The overall non-supercell data was tested for comparison purposes. The t-statistics and t-thresholds were calculated based on a desired 90% confidence and are depicted in Table 5.

Freezing Level (ft)	Number of Storms (n)	t-threshold	t-statistic	Mean Residual	Reject Null Hypothesis
<9500	29	1.701	0.14	0	No
11500–12500	20	1.729	0.17	-4.26E-14	No
>14500	78	1.664	1.44	-4.55E-13	No
Total	308	1.285	4.68	-1.36E-12	Yes

Table 5. Hypothesis test for null hypothesis that the slope between hail size and storm-top divergence is less than or equal to zero. Values recorded include the number of storms, t-threshold, t-statistic, mean residual values, and result of hypothesis test.

Based on the values in Table 5, the null hypothesis should not be rejected for each freezing level as the t-statistic is less than the t-threshold. Thus uncertainty still surrounds the relationship between hail size and storm-top divergence for these three freezing level ranges. But in the case of the total sample, the t-statistic is larger than the t-threshold value, further proving a positive correlation between hail size and storm-top divergence exists for non-supercell thunderstorms. Examination of the residual values indicates that the mean residual value is approximately zero within each freezing level category. This implies that the residual values are due to random error and not some other factor.

Since a correlation can be stated with 90% confidence for all measurements, but not for the individual freezing level categories of <9500, 11500–12500, and >14500 feet, a larger sample size is required within each of these categories. The distribution of hail sizes per freezing level height is depicted in Table 6. The <9500 and 11500–12500 categories contain the least amount of hail reports and would benefit from larger sample sizes. The >14500 category contains the most reports of all the categories, however while some hail sizes are well represented, others are not. Only one report was recorded in two of the larger hail categories, which would likely alter the results. In fact, the same

problem arose in other freezing level categories, albeit having high confidence in the positive hail size to storm-top divergence correlation. Thus all the designated freezing level categories would benefit from an increased sample of hail reports of all hail sizes.

Freezing Level (ft)	0.75”	0.88”	1.0”	1.25”	1.5”	1.75”	≥2.0”	Total
<9500	11	8	6	0	2	2	0	29
9500–10500	18	16	14	9	2	5	2	66
10500–11500	4	13	10	4	4	3	0	38
11500–12500	3	1	5	2	3	4	2	20
12500–13500	7	7	4	1	12	0	1	32
13500–14500	15	12	9	4	1	3	1	45
>14500	17	27	19	4	1	9	1	78
Total	75	84	67	24	25	26	7	308

Table 6. Distribution of hail size reports within the seven freezing level categories.

E. WET-BULB ZERO

In addition to the freezing level, the wet-bulb zero height was measured and analyzed for correlations between hail size and storm-top divergence. The data collected in Tables 7 and 8 indicate that the largest hail size occurs when the wet-bulb zero height is between 10500 and 11500 feet. As with the freezing level, the maximum and minimum hail sizes recorded do not offer much information in terms of wet-bulb zero height importance. With the exception of the 10500–11500 category, the average storm-top divergence was stronger when the wet-bulb zero height was greater, which correlates to the increase in the average surface temperature and dew point. The latter two values are an indication of stronger instability due to the presence of warmth and moisture within the boundary layer.

A scatter plot of all non-supercell hail reports separated by wet-bulb zero height is shown in Figure 23. Although the linear trend line is positive for the combined wet-bulb zero height as seen in Figure 23.f, both the individual plots of <9500 and 11500–12500 depict a negatively sloped linear trend line, as depicted in Figure 23.a and 23.d. Regression analysis was performed to further explore the correlation between hail size

and storm-top divergence for a given wet-bulb zero height. The breakdown of storm totals and hail size by wet-bulb zero height is shown in Table 7. The average storm-top divergence and surface temperature and dew point are shown in Table 8. Lastly, the regression analysis is depicted in Table 9.

Wet-Bulb Zero Height (ft)	Number of Storms	Ave. Hail Size (in)	Max. Size (in)	Min. Size (in)
<9500	49	0.97	1.75	0.75
9500–10500	77	1.06	3.00	0.75
10500–11500	60	1.15	1.75	0.75
11500–12500	44	1.09	2.00	0.75
>12500	78	1.02	2.50	0.75

Table 7. Distribution of wet-bulb zero heights and their respective number of storms and average, maximum, and minimum hail sizes

Wet-Bulb Zero Height (ft)	Ave. Hail Size (in)	Ave. Storm-Top Divergence (KT)	Ave. Temp. (C)	Ave. Dew Point (C)
<9500	0.97	54	24	15
9500–10500	1.06	58	23	15
10500–11500	1.15	68	28	20
11500–12500	1.09	66	27	19
>12500	1.02	67	27	20

Table 8. Distribution of wet-bulb zero heights and their respective average hail sizes, storm-top divergence, temperatures, and dew points.

Wet-Bulb Zero (ft)	Number of Storms	Hail vs. Storm-Top Divergence Slope	Lower 90% Confidence Interval	Upper 90% Confidence Interval
<9500	49	-5.88	-20.46	8.71
9500–10500	77	10.93	4.11	17.74
10500–11500	60	16.52	3.79	29.25
11500–12500	44	-3.83	-19.82	12.16
>12500	78	30.77	19.58	41.96
Total	308	14.12	8.84	19.40

Table 9. Correlation between hail size and storm-top divergence for each freezing level category. Slope and confidence interval is depicted for each category and all categories combined

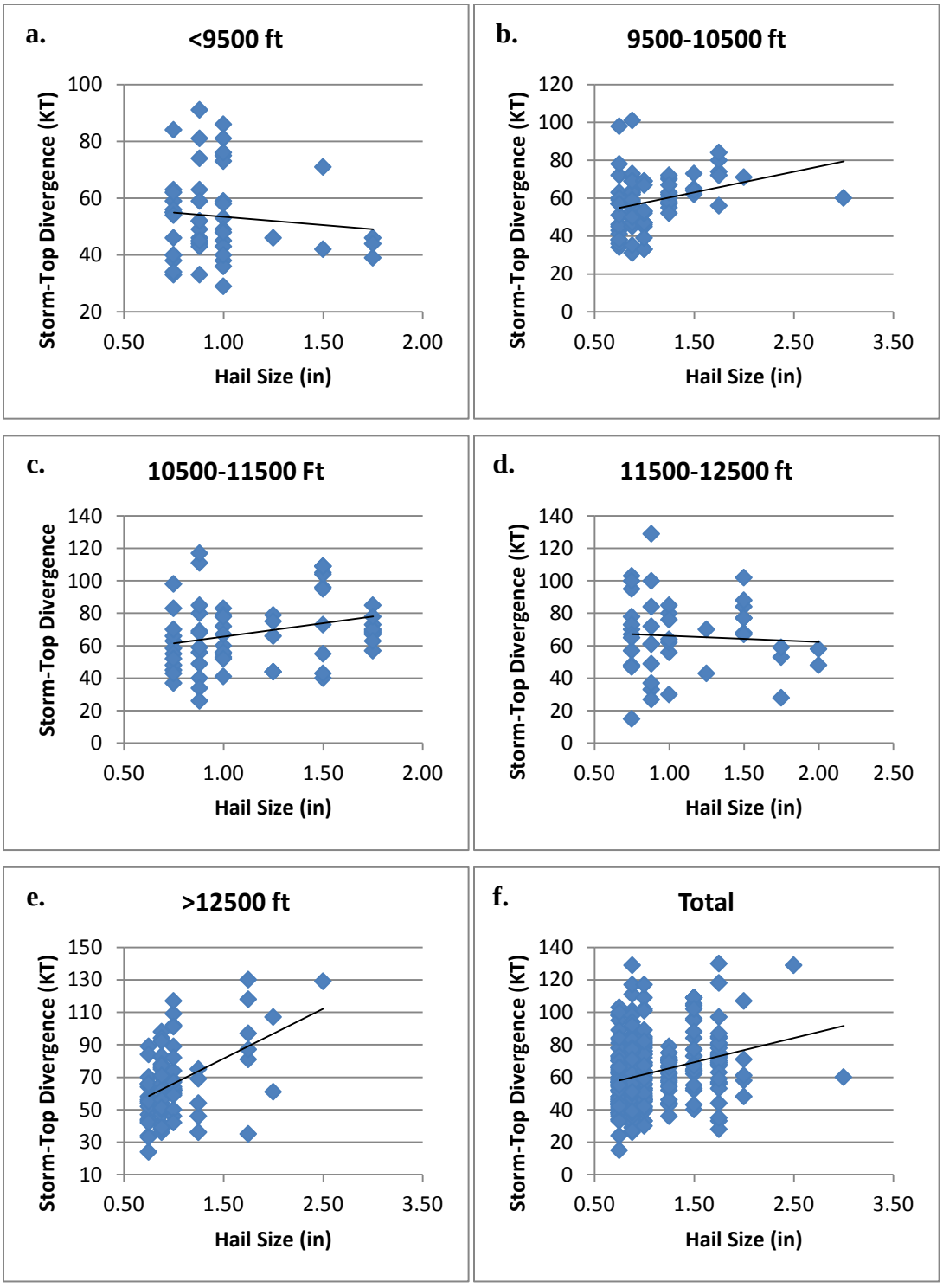

Figure 23. Scatter plots of each hailstone size with a linear trend line plotted. The plots are separated by wet-bulb zero height: (a) < 9500 ft, (b) 9500–10500 ft, (c) 10500–11500 ft, (d) 11500–12500 ft, (e) 12500–13500 ft, and (f) total.

The sign of the slopes provided by the regression analysis match the linear trend lines plotted in Figure 23.a through 23.f. Each of the slopes that were positive were also accompanied by 90% confidence. The negative slopes for the <9500 ft and 11500–12500 categories had confidence intervals that included both positive and negative values, indicating a lack of confidence in the reported negative slope. Null hypothesis testing for these two cases would be based on the slope being negative or zero. Table 10 depicts the t-threshold, t-statistic, and the mean residual value for storm-top divergence.

Wet-Bulb Zero (ft)	Number of Storms	t-threshold	t-statistic	Mean Residual	Reject Null Hypothesis
<9500	49	1.68	-0.68	7.82E-14	No
11500–12500	44	1.68	-0.40	-4.26E-14	No
Total	308	1.285	4.68	-1.36E-12	Yes

Table 10. Hypothesis test for null hypothesis that the slope between hail size and storm-top divergence is less than or equal to zero. Values recorded include the number of storms, t-threshold, t-statistic, mean residual values, and result of hypothesis test.

Wet Bulb Zero (ft)	0.75”	0.88”	1.00”	1.25”	1.50”	1.75”	≥2.00”
<9500	14	13	16	1	2	3	0
9500–10500	18	22	14	11	5	5	2
10500–11500	12	12	11	5	11	9	0
11500–12500	13	10	7	2	7	3	2
>12500	18	27	19	5	0	6	3
Total	75	84	67	24	25	26	7

Table 11. Distribution of hail size reports within the five wet-bulb zero categories.

The results of the null hypothesis show that the two negative sloped correlations could not be rejected, thus the possibility remains that positive correlation does exist between hail size and storm-top divergence at these wet-bulb zero heights. However, the total sample depicts an overall positive correlation accepted within a 90% confidence interval. As with the freezing level categories, the correlation between storm-top divergence and hail size was not necessarily stronger when wet-bulb zero was factored

into the regression. A larger sample size is desired for the <9500 and 11500–12500 categories to re-analyze the likely correlation between storm-top divergence and hail size. The distribution of hail sizes per wet-bulb zero height is depicted in Table 11.

F. TEMPERATURE AND DEW POINT

Regression analysis for all non-supercell hail reports was conducted for temperature and dew point against hail size and storm-top divergence, the results of which are depicted in Table 12. The regression slope indicates that there is a positive relationship between both surface temperature and dew point and the resulting storm-top divergence with 90% confidence, indicating that surface temperature and dew point have an effect on updraft strength However, the slope between both the surface temperature and dew point and the resulting hail size is approximately zero, indicating that surface temperature and dew point do not have a specific correlation to the resulting hail size. While increased surface temperature and dew point likely will result in stronger thunderstorm updrafts, feasibly the freezing level height and wet bulb-zero height will also increase. As shown previously in this chapter, hail size produced by the increasing storm-top divergence is offset by the increased freezing level and wet-bulb zero heights.

Regression	Slope	Lower 90% Confidence Interval	Upper 90% Confidence Interval
Temp vs. Hail Size	-2.81E-03	-9.97E-03	4.35E-03
DP vs. Hail Size	2.38E-03	-6.99E-03	1.18E-02
Temp vs. Storm-Top Div.	0.51	0.095639	0.917932
DP vs. Storm-Top Div.	1.16	0.629021	1.689839

Table 12. Hypothesis test for null hypothesis for temperature and hail size, dew point and hail size, temperature and storm-top divergence, and dew point and storm-top divergence.

G. LIFE CYCLE OF A MULTICELL THUNDERSTORM

To better understand the duration of an individual cell within a multicell thunderstorm, one storm was analyzed from the initiation of the hail producing cell until a new cell developed and the hail producing cell dissipated. This storm moved across the state of New York on 15 Jun 2009, captured by the KENX National Weather Service

radar, and produced hail of 1.0 inches. The official storm report time was 2012 UTC. The radar scans are depicted in Figures 24, 25, 26, and 27.

The 1941 UTC radar reflectivity scan shown in Figure 24.a depicts the multicell storm that produced the eventual hail report. The cell that produced the hail, indicated by the white circle, is in the developmental phase. The corresponding radial velocity scan at 5.1 degrees is shown in Figure 26.a. The white circle is transposed from Figure 24.a, indicating that the top of the storm was not yet high enough to be penetrated by the 5.1 degree radar pulse. The 5.1 degree elevation scan does pierce the cell in the following two scans, indicating that the cell intensified over the following nine minutes. By Figure 26.d, the storm top is evident on the 6.4 degree elevation scan, which is the extent of storm top evidence throughout the remaining scans.

The strongest storm-top divergence measured throughout the entire series of scans occurred on the 1950 UTC scan, 22 minutes prior to the official hail report time. This value, measured at 60 knots, was observed on the 5.1 degree elevation scan as the storm top was not yet present on the 6.4 degree scan. Based on the average hail size from all non-supercell storm-top divergence values between 55 and 64 knots, the predicted hail size would have been 1.05 inches.

As the storm-top continued to the next elevation scan, the measured divergence peaked at 45 knots and was measured as such for two subsequent radar scans. From all non-supercell storms, the average hail size for storm top divergence between 45 and 54 knots was 0.96 inches. By 2008 UTC, as shown by the reflectivity scan on Figure 25.a, a new cell began to develop southwest of the hail producing cell, indicating that the original cell had already reached maturity and dissipation began. This is confirmed by the divergence pattern depicted on Figure 27.a as a secondary divergence signature developed to the southwest of the originally followed divergence pattern. The life cycle of the hail producing cell was approximately 40 minutes before being asphyxiated by the newly developed cell of the multicell storm structure.

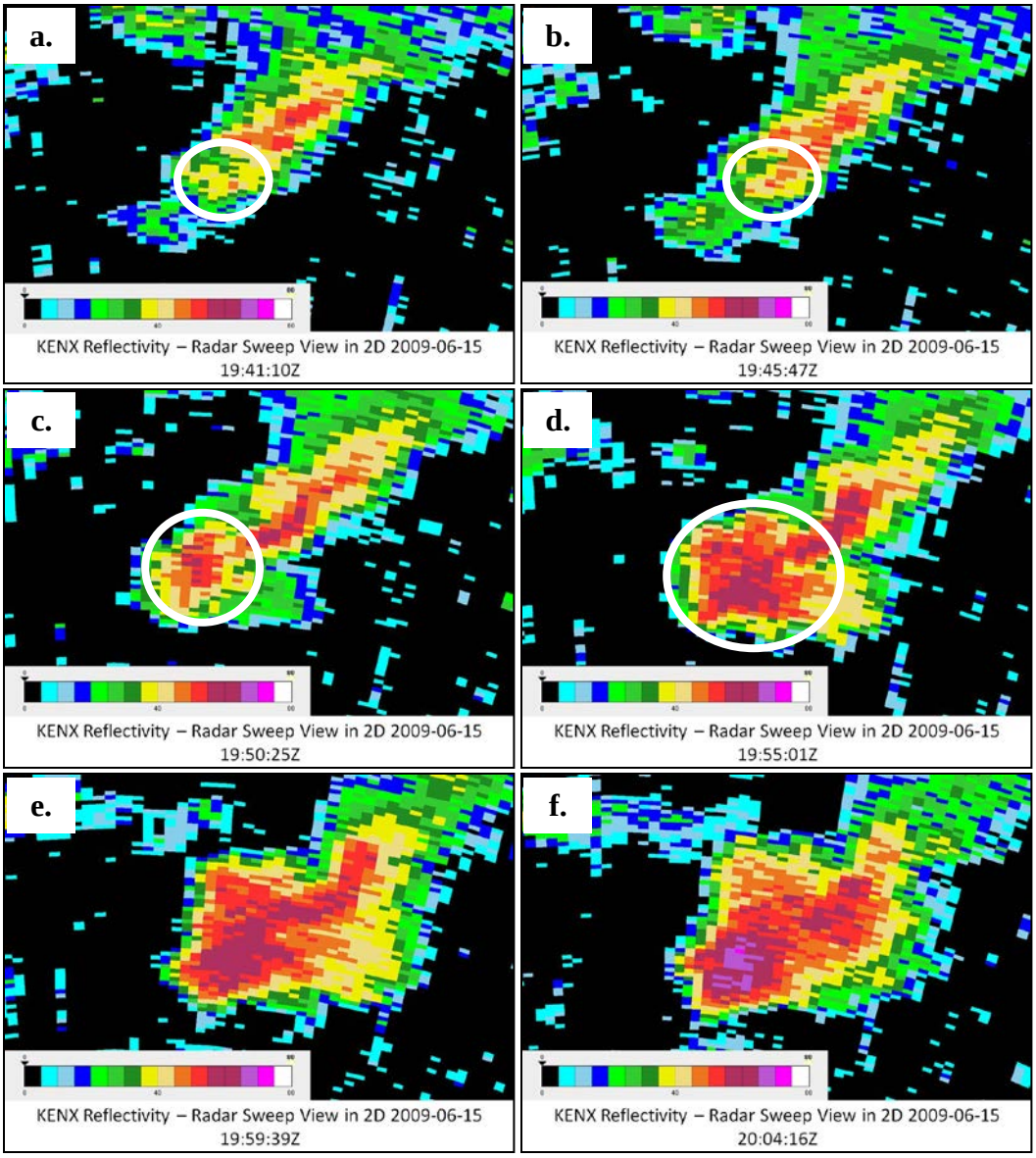

Figure 24. Radar reflectivity scans on 15 Jun 2009 from KENX radar in Albany, NY. The scans were taken at (a) 1941 UTC, (b) 1945 UTC, (c) 1950 UTC, (d) 1955 UTC, (e) 1959 UTC, and (f) 2004 UTC.

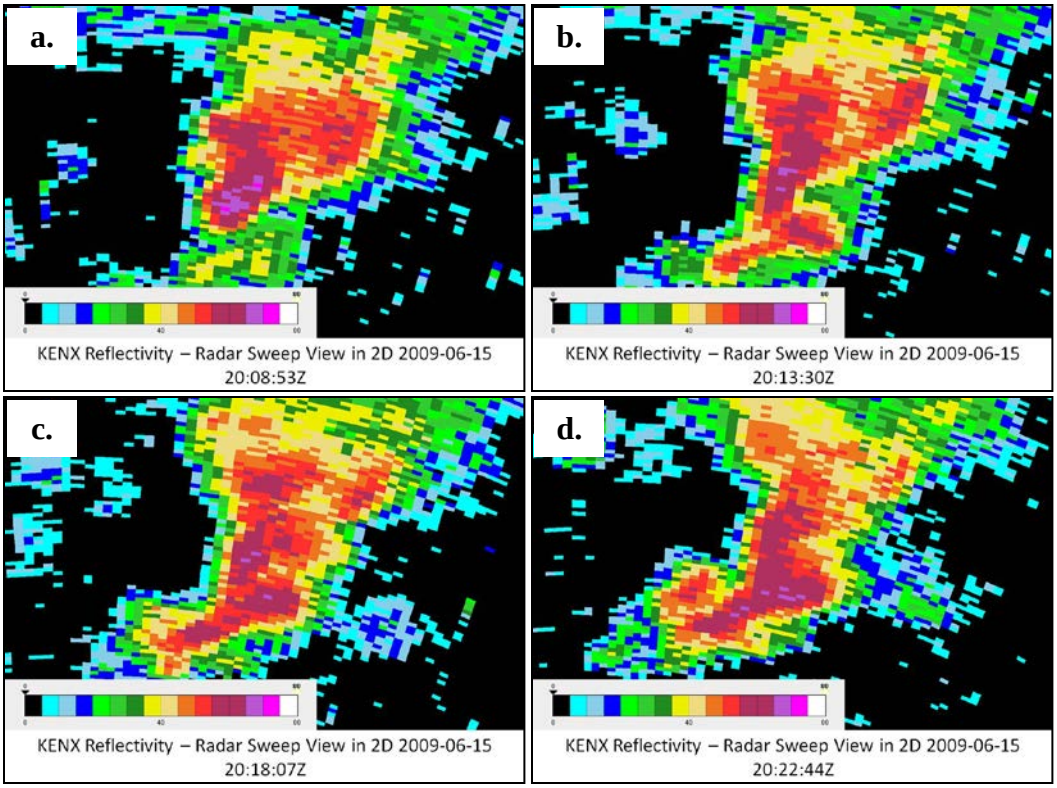

Figure 25. Radar reflectivity scans on 15 Jun 2009 from KENX radar in Albany, NY. The scans were taken at (a) 2008 UTC, (b) 2013 UTC, (c) 2018 UTC, and (d) 2022 UTC.

For this particular example, Boustead's specification for analysis, interrogating all radar scans 15 minutes prior to and five minutes after the storm report, would have missed the maximum storm-top divergence as the highest value was observed 22 minutes before the storm report. Both Boustead's method and the one used in this thesis would have captured the 45 knot value that occurred within ten minutes of the storm report time. However, if the averages from this study were used as a baseline for forecasting hail size, then the predicted 0.96 inches was less than 0.05 inches from the observed 1.0 inches. If the 65 knot storm-top divergence was to be observed by a forecaster, then 1.05 inches would have been predicted, only 0.05 inches larger than the actual report.

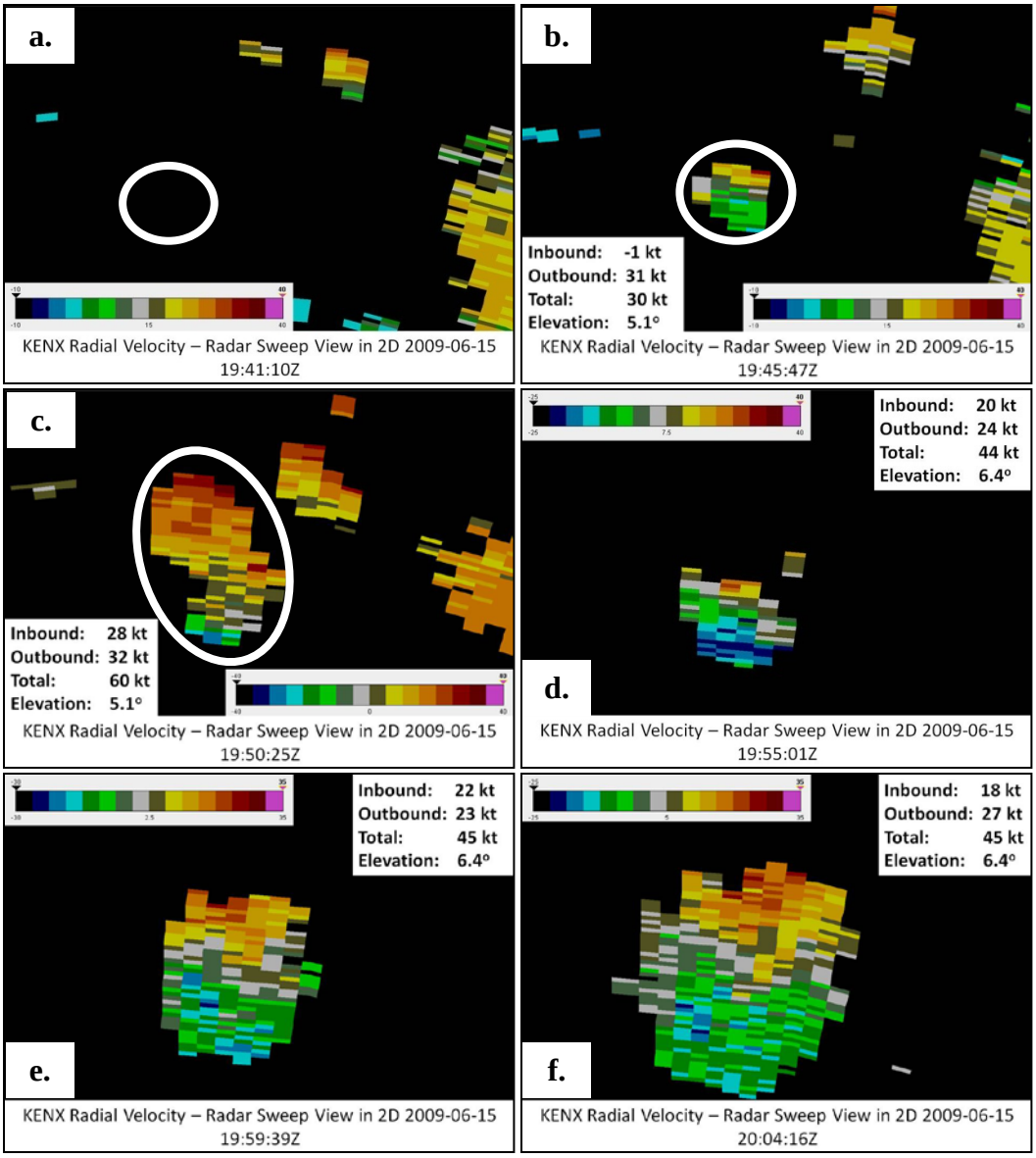

Figure 26. Radar radial velocity scans on 15 Jun 2009 from (b) 1945 UTC, (c) 1950 UTC, (d) 1955 UTC, (e) 1959 UTC, and f) 2004 UTC.

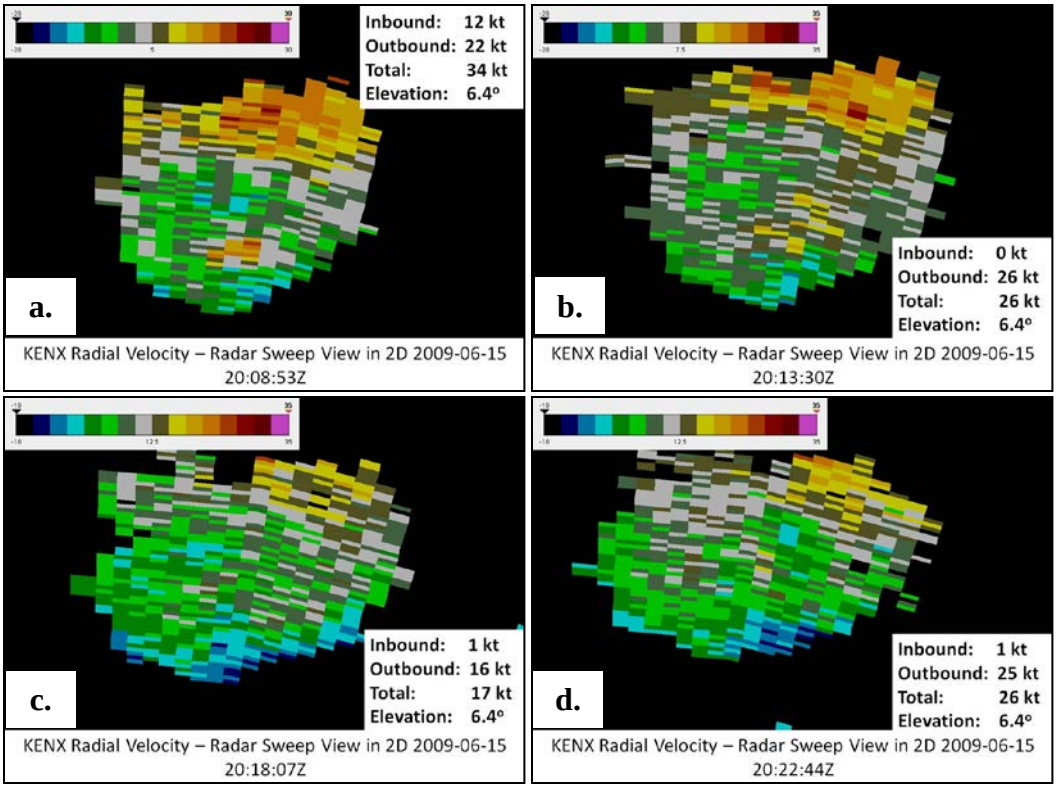

Figure 27. Radar radial velocity scans on 15 Jun 2009 from KENX radar in Albany, NY. The scans were taken at (a) 2008 UTC, (b) 2013 UTC, (c) 2018 UTC, and (d) 2022 UTC.

As noted in Chapter II, the duration of an individual cell of a supercell can be upwards of three hours, while the cell shown in this case study lasted roughly 40 minutes. The average time between scans was 4.6 minutes. It is feasible that the maximum storm-top divergence occurred sometime between the scans and would be missed by operational forecasters. Although the maximum storm-top divergence did occur prior to the hail report, suggesting that storm-top divergence can be a useful nowcast tool for predicting hail size.

THIS PAGE INTENTIONALLY LEFT BLANK

V. CONCLUSIONS AND RECOMMENDATIONS

A. CONCLUSIONS

There is a strong relationship between hail size and the strength of the thunderstorm updraft, which can be deduced from measured storm-top divergence. This relationship has been extensively studied within supercell thunderstorms and was proven in this study by regression analysis of all non-supercell thunderstorms and their respective storm-top divergence values. However, since supercells are dynamically different from non-supercell thunderstorms, the previously established correlation should not be used when the focus is on non-supercells.

1. Hail Size and Storm-Top Divergence

Individual updraft duration within a non-supercell thunderstorm is typically much shorter than that of the updraft in a supercell. The average updraft duration for an individual cell within a multicell thunderstorm is 30 minutes, much shorter than the average three hour duration of a supercell updraft. The hail producing cell of one of the multicell thunderstorms in this study lasted approximately 40 minutes before dissipating in the wake of new cell development. A long lasting updraft will have more time to intensify before dissipation and more time to keep growing hailstones suspended in subfreezing temperatures. Of the thunderstorms analyzed in this study, 2.0 inch or greater hail accounted for 2.7% of the non-supercells reports and 12.5% of supercells reports. Roughly 75% of non-supercells and 60% of supercells produced hail of 1.0 inches or less. Both sets of numbers indicate that a higher percent of non-supercells produce small severe hail while supercells are more apt to generating large severe hail.

The maximum storm-top divergence measured over the course of this study was 130 knots. Boustead's forecast table was constructed with the means to forecast hail produced from storm-top divergence values of up to 231 knots. Based on the results of this study, updraft intensity of non-supercell thunderstorms is typically not strong enough to produce extremely high levels of storm-top divergence. These results are consistent

with thunderstorm parameters in the Northeastern U.S. where the average summer time tropopause height is lower than that of the Great Plains. Higher tropopause heights allow for taller and stronger updrafts, resulting in higher measured storm-top divergence values.

Additionally, Boustead's forecast table did not provide guidance for measured storm-top divergence values less than 55 knots. One-hundred twelve of the 308 severe hail producing non-supercell storms from this research had measured storm-top divergence values less than 55 knots with an average hail size of 0.96 inches. As Boustead's research utilized supercells and multicells from the Great Plains, the average storm-top divergence values from his research would be higher than that of multicell thunderstorms observed over the Northeastern U.S.

2. Freezing Level and Wet-Bulb Zero Height

Since varying freezing level heights alter the duration in which hail falls through air above freezing temperatures, regression analysis was applied to seven separate thousand foot freezing level categories. The results indicated a positive correlation between hail size and storm-top divergence within each category, although three of the seven categories were not supported by a 90 percent confidence interval test and null hypothesis testing. This means that further proof is required to state that positive relationship exists when the freezing level is incorporated.

The same analysis was applied to five separate thousand foot categories of wet-bulb zero heights. Three of the five categories displayed a positive correlation between hail size and storm-top divergence with 90% confidence in the relationship. However, regression analysis of two of the categories resulted in a negative correlation. Confidence was low with these results, indicating that the relationship may in reality be positive. However, further testing is required before that assumption can be made, thus the results of this research cannot prove that adding wet-bulb zero heights to measured storm-top divergence would improve the established correlation to hail size.

3. Temperature and Dew Point

Regression analysis was conducted on observed temperature and dew point values against both hail size and storm-top divergence. The regression slope calculated for the relationship between temperature and hail size was approximately zero. The calculated slope for dew point and hail size was also approximately zero. Both of these results indicate that there is no proportionality relationship between the surface temperature or dew point and the resulting hail size.

However, a positive correlation was revealed when regression analysis was applied to the relationship between surface temperature and storm-top divergence. A stronger positive relationship was discovered from the regression analysis between dew point and storm-top divergence. When both the surface temperature and dew point are increased the atmosphere is typically more unstable, which would account for stronger storm-top divergence values. However, since there was no hail size relationship, increasing surface temperatures and dew points also infers higher freezing level heights due to increased atmosphere thickness, which has already been shown to allow for higher storm-top divergence values. Thus incorporating temperature and dew point to observed values of storm-top divergence will not improve the correlation to hail size.

B. RECOMMENDATIONS

The relationship between hail size and storm-top divergence has been explored over the Northeastern U.S. However, the results from this thesis reveal that further study is required. Although it has been proven that there is an overall correlation between measured storm-top divergence and the resulting hail size from non-supercell thunderstorms, more research should be accomplished within each thousand foot freezing level and wet-bulb zero category as sample sizes were actually quite small when all of the parameters were put in place. To increase the sample size, more storm reports for each hail size should be obtained within each freezing level and/or wet-bulb zero category, specifically in the categories where confidence could not assure the positive relationship between storm-top divergence and hail size.

This study's focus was on the Northeastern U.S. As non-supercell thunderstorms occur all over the United States, future studies should explore other geographical regions of the United States. Differing regions would likely produce different storm-top divergence values due to varying average heights of the freezing level and tropopause.

In addition to the synoptic cases of this study, other synoptic situations should be explored. Since most of the cases in this study were produced by low pressure systems originating from Canada, similar atmospheric conditions were present for all of the thunderstorms. The correlations discovered in this thesis may not apply to other synoptic situations. Low-pressure systems that originate from other regions of the United States may yield different results due to a change in dynamic or thermodynamic conditions, such as stronger cold fronts, stronger upper-level jets, or increased surface moisture in the warm sector of the low.

This study focused on non-supercell thunderstorms, including bow echoes, multicells, and squall-lines. However, further study into each type of storm individually would possibly yield different results as these storm types differ dynamically from each other. Furthermore, single-cell thunderstorms were not explored in this research as none occurred due to the chosen synoptic situations. While single-cell storms do not typically produce severe weather, they have been known to produce severe hail and winds. Results may be similar to those of this study as the individual cells explored here have similar duration times to that of a single-cell thunderstorm, although cell dissipation in a single-cell storm occurs when mass at the top of the thunderstorm becomes too great for the updraft to support, differing from the main reason cells dissipate in multicell storms. Further research into the dynamic relationship between hail size and storm-top divergence is warranted.

The individual multicell storm case that was studied from cell inception to dissipation revealed that the strongest measured storm-top divergence was observed at a lower radar elevation angle prior to the storm top reaching maximum altitude. When the cell reached its peak altitude and was interrogated by a higher radar elevation scan, the measured storm-top divergence decreased. As the cell increased in height, the cell is maturing, thus measured storm-top divergence ideally should be strongest when the cell

peaks in intensity. However, as radar elevation angles increase, the measured horizontal radial velocities decrease. Therefore, a future study should investigate the extent of the affect of radar elevation angle on the measured radial velocity.

Additionally, Level III data should be used for further research to remove the affect of Velocity Folding on the velocity data. Storms analyzed in this study may have actually contained larger values of storm-top divergence than what was recorded and storms that were discarded may have been acceptable for analysis. Since NCDC does not archive all the elevation angles of Level III radar data, the data must be archived by the researcher as the storms occur, compiling the data over time.

Lastly, this study should be re-accomplished when a phased array radar network replaces the current NWS WSR-88D network. Current radar scans take up to five minutes to complete as the radar scans each elevation angle in succession, as shown in the analysis of the 15 Jun 2009 New York multicell thunderstorm. Rapidly changing conditions within a thunderstorm may be missed as the WSR-88D scans other levels of the thunderstorm. Phased array radar scans all levels at once and would be able to capture rapidly changing conditions as they happen. Instances where maximum storm-top divergence occurs between radar scans would no longer be an issue. The same dataset for this study would be more accurate and error would be reduced, having less of an effect on the results.

THIS PAGE INTENTIONALLY LEFT BLANK

LIST OF REFERENCES

Beebe, R. G. and Bates, F. C., 1955: A Mechanism for assisting in the release of convective instability. *Mon. Wea. Rev.*, **83,** 1–10.

Boustead, J. M., 2008: Using maximum storm-top divergence and the vertical freezing level to forecast hail size. Preprints, *24th Conference on Severe Local Storm*, P6.6, Savannah, GA, National Weather Service, 5 pp.

Chaston, P. R., 1999: *Thunderstorms, Tornadoes, and Hail!* Chaston Scientific, Inc., 224 pp.

Donavon, R. A. and Jungbluth, K. A., 2007: Evaluation of a technique for radar identification of large hail across the upper Midwest and central Plains of the United States. *Wea. and Forecasting*, **22**, 224–254.

Doswell, C. A. III, 2001: Severe Convective Storms -- An Overview. *Severe Convective Storms*, Charles A. Doswell III, American Meteorological Society, 1–13.

Fawbush, E. J. and Miller, R. C., 1951: An Empirical Method of Forecasting Tornado Development. *Bulletin of the American Meteorological Society*, **32**, 1–9

Lemon, L. R., and D. W. Burgess, 1980: Magnitude and implications of high speed outflow at severe storm summits. Preprints, *19th Conf. Radar Meteor. Conf*., Boston, MA, Amer. Meteor. Soc., 364–368.

National Weather Service, cited 2012: National Weather Service Glossary. [Available online at http://www.weather.gov/glossary/]

Snapp, M. R., 1979: Investigation of the single Doppler divergence signatures as an objective severe hailstorm detection method. M.S. thesis, School of Meteorology, University of Oklahoma, 47 pp.

Weisman, M. L. and Klemp, J. B., 1986: Characteristics of Isolated Convective Storms. *Mesoscale Meteorology and Forecasting*, Peter S. Ray Ed., American Meteorological Society, 331–358.

Ziegler, C. L., Ray, P. S., and Knight, N. C., 1983: Hail Growth in an Oklahoma Multicell Storm. *J. Atmos. Sci.*, **40**, 1768–1791.

THIS PAGE INTENTIONALLY LEFT BLANK

INITIAL DISTRIBUTION LIST

1. Defense Technical Information Center
   Ft. Belvoir, Virginia

2. Dudley Knox Library
   Naval Postgraduate School
   Monterey, California

3. Allison Wreath
   15th Operational Weather Squadron
   Scott Air Force Base, Illinois

4. Wendell A. Nuss
   Monterey, California

5. Michael M. Bell
   Monterey, California

6. Department of Meteorology
   Naval Postgraduate School
   Monterey, California

7. Petrit J. Hasa
   28th Operational Weather Squadron
   Shaw Air Force Base, South Carolina